The Impact of Selected Gene Mutations to the Activation and DNA Binding Activity of the Transcription Factor VraR

Ghazal Tajbakhsh

A THESIS SUBMITTED TO
THE FACULTY OF GRADUATE STUDIES
IN PARTIAL FULFILLMENT OF THE REQUIREMENTS
FOR THE DEGREE OF MASTER OF SCIENCE

GRADUATE PROGRAM IN BIOLOGY

YORK UNIVERSITY

TORONTO, ONTARIO

March 2017

ABSTRACT

VraSR two-component system in *S. aureus* senses bacterial cell wall damage caused by antibiotics (vancomycin or β-lactams) and regulates a set of genes. We have undertaken the study of the role of certain amino acids in the function of VraR, which undergo mutation in clinical *S. aureus* resistant strains and analyzed their effects on the VraSR signal transduction mechanism. In particular, we have looked at the role of Met-13 in VraR phosphorylation induced activation. M13A failure to be activated by phosphorylation resulted in a weaker binding to DNA. Moreover, we investigated VraR E59D, S164P, A113V, and S164A binding activity to the P*vraSR* by DNase-I footprinting. Finally, *in vivo* studies on the effects of substitutions of the above residues on the mRNA level of a number of VraSR regulon genes (*fmtA, pbp2, and sgtb*) provide insights as to how substitutions at certain positions may be beneficial to the *S. aureus* resistance to antibiotics.

ACKNOWLEDGMENTS

This acknowledgment will briefly look into all individuals who have partaken on this journey with me in one way or another, persons whom I could not have done this without.

I cannot ever forget the first day that my supervisor Dr. Dasantila Golemi-Kotra permitted me to work in her lab. I am super flattered to have been recommended this topic of choice by my professor and humbled to have progressed this far, acquiring vast amounts of information along the way.

My professor did not hesitate one bit at any one point to direct me towards the right path. She essentially paved the way for the blossoming of my interest in this field, and I am massively grateful for that. She taught me that persistence is what carries one to newer and greater heights.

I truly express my gratitude for committee members Dr. D. Wilson, Dr. M. Scheid, and my committee chair and advisor, Dr. Yi Sheng for their wise and helpful constructive criticism throughout the course of my thesis. Also, I have been lucky to work side by side with such wonderful lab colleagues, including, but not limited to, Maryan Mohiadin, Mayoorey Murugathasan, Uzma Muzamal, and especially Shailee Jani who have made this experience all worthwhile.

Most crucial of all, a huge shout-out goes to my family especially my parents who have been so supportive and patient with my ongoing learning process, and have motivated and borne with me through all the ups and downs.

There is no one more deserving to whom I would like to dedicate this thesis: my late grandfather, ‘Papoochka.’

Constant dropping wears away a stone.

TABLE OF CONTENTS

LIST OF TABLES

LIST OF FIGURES

CHAPTER ONE

CHAPTER TWO

LIST OF ABBREVIATIONS

Ala (A)	Alanine
B. subtilis	*Bacillus subtilis*
CA	Catalitic Domain
ED	Effector domain
E.coli	*Escherichia coli*
HTH	Helix-turn-helix
HK	Histidine kinase
DHp	Histidine Phosphotransfer Domain
LB	Luria-Berani Broth
MRSA	Methicillin-resistant *S. aureus*
PCR	Polymerase Chain Reaction
PBPs	Penicillin-binding proteins
PBP2a	Penicillin-binding protein 2a
PRSA	Penicillin-resistant staphylococci
PGTs	Peptidoglycan glycosyltransferases
qRT-PCR	Real Time Quantitative Polymerase Chain Reaction
REC Domain	Receiver domain
VraSR	TCS resistance to vancomycin in *S.aureus*
VanSR	TCS resistance to vancomycin in *Enterococcus faecium*
LiaSR	TCS resistance to bacitracin in *B.subtilis*
RR	Response regulator

SDS-PAGE	SDS-polyacrylamide gel electrophoresis
SCCmec	*Staphylococcal* Cassette Chromosome mec
SFD	Staphylococcal foodborne disease
S. aureus	*Staphylococcus aureus*
TPs	transpeptidases
TSB	Tryptic Soy Broth
TCSs	Two component systems
TCRSs	Two component regulatory systems
VRSA	Vancomycin-resistant *S. aureus*
VISA	Vancomycin Intermediate *S. aureus*
VraR-P	Phosphorylated VraR
VSSA	Vancomycin Susceptible *S. auresus*

1 CHAPTER ONE: S. AUREUS TWO-COMPONENT SYSTEM

1.1 *Staphylococcus aureus* properties and pathogenicity

Staphylococcus aureus (*S. aureus*), a Micrococcaceae family member is a gram-positive bacterium, which can appear as grape-shaped clusters under the microscope. *S. aureus* has round, large, and golden-yellow colonies (Ryan K.J, *et al*, 2004; Lowy F.D, 1998). *S. aureus* cell wall is a vital structural element in stress-bearing and shape-maintaining. It consists of cross-linked peptidoglycan (PG) chains via peptide bridges. The main unit of PG is a disaccharide-pentapeptide such as N- acetylglucosamine and N-acetylmuramic that is connected by glycosidic bonds. This pentapeptide is covalently connected to the lactyl group of the muramic acid such that its composition is varied among bacteria. In both *Bacillus subtilis* (*B. subtilis*) and *Escherichia coli* (*E. coli*), the dibasic amino acid of the peptide is *meso*-diamoinopimelic acid, whereas in *S. aureus* it is *L*- lysine, to which a penta-glycine linked bridge is bound (Figure 1.1). PG chains have a maximum of 20 to 26 disaccharide units making a thick cell wall also containing teichoic acid and teichuronic acid as well as some proteins (Scheffers D, *et al*, 2005).

S. aureus is normally found as a commensal bacterium associated with skin and mucosal membranes, especially in the nasal passages of healthy individuals. However, it can act as a human pathogen by colonizing in the anterior nares sites. Patients with *S. aureus* infections are normally infected with a similar strain as their commensal. *S. aureus* is one of the major sources of hospital and community-acquired infections, due to typically compromised immune system in patients (Diekema D, *et al.*, 2001; Plata K, *et al*, 2009).

Nosocomial *S. aureus* infections affect the skin, bloodstream, and respiratory tract. It can be a cause of bacteremia, pneumonia and sepsis, and even deep-rooted infections such as endocarditis and osteomyelitis (Foster TJ, 1991; Schito G, 2006). Moreover, *S. aureus* is often responsible for toxin-mediated diseases such as toxic shock syndrome, staphylococcal foodborne disease (SFD), and scalded skin syndrome (Lindsay J.A, & Holden M.T, 2004).

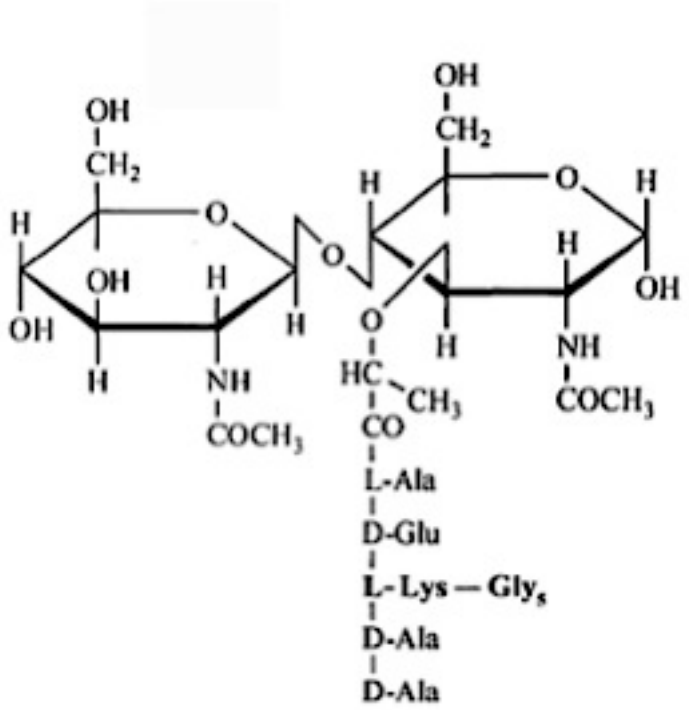

Figure 1. 1 Peptidoglycan basic unit structure is taken from Scheffers and G. Pinho, (2005).
Disaccharide-pentapeptide is the basic unit of the *S. aureus* cell wall peptidoglycan.

1.2 Antibiotic resistance in *S. aureus*

1.2.1 Penicillin-resistant S. aureus

The origin of antibiotics and antibiotic-resistance in *S. aureus* goes back to 1941, when penicillin was first introduced to clinical practice. Penicillin was the first antibiotic, produced by *penicillium*, a mold, which was discovered by a Scottish scientist, Alexander Fleming in 1928 (Grundmann H, 2006). In 1942, two years after penicillin introduction, the first series of penicillin-resistant staphylococci (PRSA) were recognized in hospitals and societies (Rammelkamp C.H, & Maxon T, 1942). The penicillin resistance in *S. aureus* is due to the *blaZ* gene function that is encoding β-lactamase. In the presence of β-lactam antibiotic, this enzyme breaks the structural ring of the antibiotic leading to its inactivation. There are two nearby regulatory genes, *blaI* (repressor) and *blaRI* (anti-repressor), which control the *blaZ* gene (Kernodle D.S, 2000). BlaRI, as a protease, hydrolyzes itself and BlaI allows *blaZ* to produce enzymes in the case of any exposure to β-lactams (Gregory P.D, *et al*, 1997; Zhang H.Z, 2001) (Figure1.2).

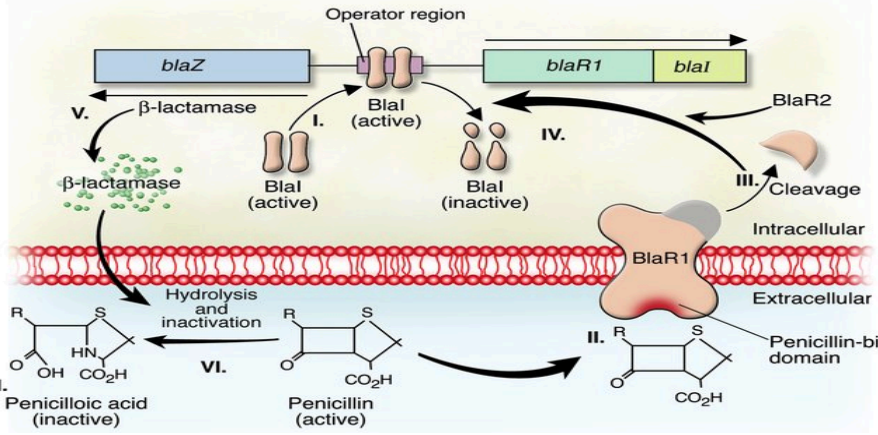

Figure 1. 2 Induction of staphylococcal β-lactamase synthesis in the presence of penicillin that is taken from Lowy FD. (2003).
I) In the presence of penicillin, BlaI binding to the operator region, represses *blaZ* and *blaRI-blaI* transcription. II) Binding of penicillin to the BlaR1 stimulates its activation. III-IV) Active BlaRI cleaves BlaI by BlaR2 assistance and lets the transcription to start. V-VII) β-lactamase encoded by *blaZ*, breaks the β-lactam ring of penicillin and causing its inactivation.

By the late 1960s, more than 60% of the *S. aureus* strains, mostly in hospitals, had acquired penicillin resistance, and 90% of *S. aureus* strains showed resistance through the production of β-lactamase (Lowy F.D, 2003). Eventually, scientists started an intense race to win the battle between resistant bacteria and significant antibiotic discovery.

1.2.2 Methicillin-resistant *S. aureus* (MRSA)

In 1959, methicillin, a semi-synthetic penicillin, was discovered to overcome the inactivation of penicillin by β-lactamase (Lowy F.D, 2003). Initially, methicillin and other β-lactams were successful in treating penicillin-resistant *S. aureus.* However, the extensive usage of methicillin was followed by reports of methicillin-resistant *S. aureus* (MRSA)

isolates as early as 1961. In 1970 MRSA had become the major cause of nosocomial infections globally and was termed "super bug."

The mechanism leading to methicillin resistance was finally identified in 1981. MRSA arose because of the acquisition of the *mecA* gene from *Staphylococcus sciuri7* (Stapleton P.D, & Taylor P.W, 2002). The 2.1-kb *mecA* codes for penicillin-binding protein 2a (PBP2a) is located on a genetic element, *Staphylococcal* Cassette Chromosome mec (SCCmec). In the presence of the β-lactam antibiotic, PBP2a affinity, which is responsible for the last step of cell wall peptidoglycan synthesis, is reduced but the cell wall biosynthesis continues developing. In this case, methicillin cannot bind to the target PBP (Ito T, *et al*., 2003).

The high occurrence of MRSA in hospitals from 1997 to 1999 was noted 66.8% in Japan, 40.4% in South America, 34.2% in Latin America and 33.4% and 26.3% in the USA and Europe. Since the emergence of MRSA, the treatment of choice was the glycopeptide vancomycin (Bell J.M, *et al.*, 2002; Diekema D, *et al.*, 2001).

1.2.3 Vancomycin-resistant *S. aureus* (VRSA)

The early 1990s showed a noticeable increase in vancomycin use in United States due to the growing numbers of infections with staphylococci strains in health care institutions. As a consequence, MRSA became resistant to the only effective antibiotic, vancomycin. The first strain of *S. aureus* with reduced susceptibility to vancomycin emerged in Japan in 1997 (Gaddad S, *et al*, 2011). Later, in 2002, vancomycin-resistant *S. aureus* (VRSA) isolates were found in the USA. No antibiotic could solely overcome their

resistance ability (Enright M, 2003). Analyzing the MRSA isolates with reduced susceptibility to vancomycin revealed a reduction in peptidoglycan cross-linking leading to high exposure of D-Ala-D-Ala residues. The reduced amount of L-glutamine responsible for amidation of D-glutamate in the pentapeptide bridge is the result of altered cross-linking (Walsh T.R, & Howe R.A., 2002). Therefore, more D-Ala-D-ala is produced to trap the applied vancomycin. Consequently, vancomycin segregates, causing a reduction of the antibiotic amount reaching to the sites of the cell wall biosynthesis that results in a thickened cell wall (Cui L, et al, 2000).

Another form of vancomycin resistance (complete vancomycin-resistant strains) is mainly due to the acquisition of foreign *vanA* operon. Thus, the *vanA* gene makes particular changes in the cell wall precursor terminal peptide of D-Ala-D-Ala to D-Ala-D-lac (Lowy F.D, 2003). The new peptide has a significant low affinity for vancomycin. Hence, future therapies and investigations may be needed to overcome this function (Figure 1.3).

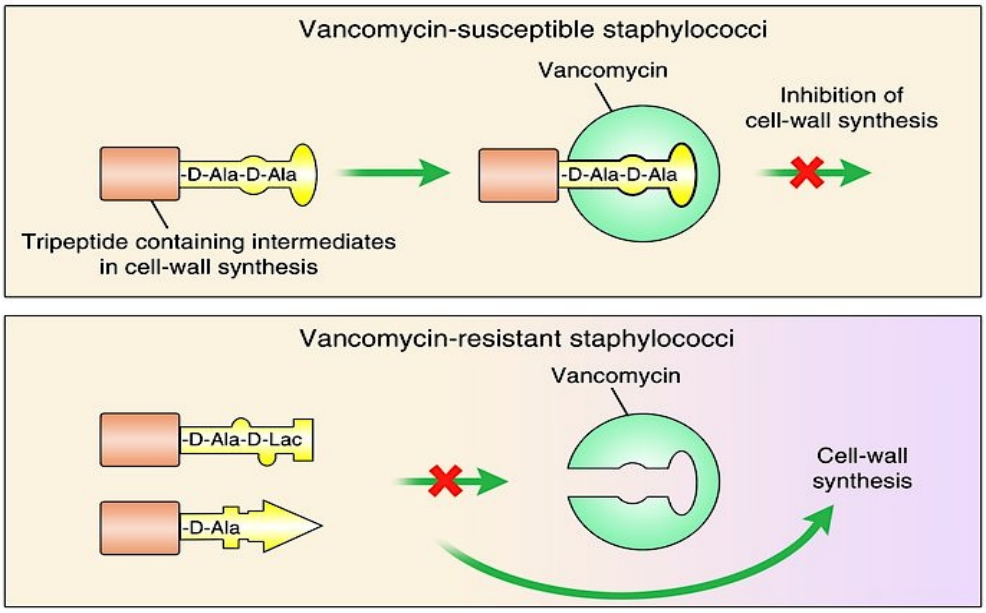

Figure 1. 3 Vancomycin resistance mechanisms in *S. aureus,* that is taken from Lowy F.D. (2003).
Upon *vanA* operon acquisition by *S. aureus,* the terminal peptide of the cell wall precursor is changed from D-Ala-D-Ala to D-Ala-D-Lac leads to vancomycin resistance by causing reduced affinity for Vancomycin.

1.3 Two component regulatory systems (TCRSs)

According to the bacterial antibiotic resistance history, this obstacle has been considered by numerous scientists who have completed research in an effort to discover a solution. One target, which has recently attracted researchers' attention, is the "two component systems" (TCSs) existing in Eubacteria, Archaea, and Eukarya (Koretke K, *et al.,* 2000). These organisms utilize sensing and signaling transduction systems to adapt to environmental stimuli. TCSs are composed of a homodimeric histidine kinase (HK) and a response regulator (RR); HKs sense external stress and transmit the related information to

the RR in a phosphorylation process. In this phosphorelay pathway, the HK is phosphorylated on a conserved histidine residue, which then transfers its phosphoryl group to the aspartic acid of the RR. In general, many phosphorylated RRs then bind to the upstream region of pathogenic genes and regulate their expression. Sometimes HK also dephosphorylate the phosphorylated RR due to its phophotranferase ability. Comparing the difference between phosphorylation and dephosphorylation determines the RR's phosphorylation state regulating gene expression (Stock AM, 2009), (Figure 1.4). TCSs could represent novel targets for the development of antibacterial agents, in particular due to their absence in animals and humans (Gotoh Y, *et al*., 2010). TCSs have been involved in antibiotic resistance, such as resistance to bacitracin in *B.subtilis*-LiaSR- (Mascher T, *et al*., 2003) and vancomycin in *Enterococcus faecium* –VanSR- (Wright G.D, *et al*., 1993) or *S. aureus* (VraSR); both, bacitracin and vancomycin are cell wall synthesis inhibitors.

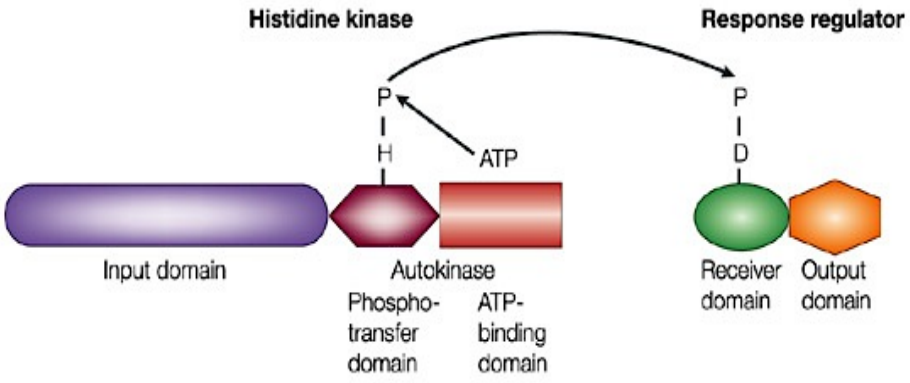

Figure 1. 4 A schematic diagram shows a simple two-component system is taken from Jensen R.B, *et al.* (2002).
The TCS consists of a histidine kinase (HK) and a response regulator (RR). Upon bacteria cell wall damage, HK senses the environment signal by activating its autokinase domain. As a result, the His residue of HK receive a phosphoryl group from ATP and then transfers it to the RR Asp residue. The active RR regulates the expression of some gene by binding to its promoter.

1.3.1 VraSR Two-component system

S. aureus has 16 pairs of two-component system, one of which is the VraSR system. The VraSR system is unique from other TCSs in that it controls the *S. aureus* reaction to inhibitors of "early and late steps" in cell wall peptidoglycan biosynthesis (Utaida S, 2003).

Briefly, the main constituent of the bacterial cell wall is peptidoglycan as its synthesis takes place in three main steps at different locations in the cell. First, the sugar-linked precursor, UDP-N-acetylmuramyl (UDP-Mur-NAc)-pentapeptide and UDP-N-acetylglucosamine (UDP-GlcNAc) are produced in the cytoplasm. Second, lipid I is formed at the cytoplasm membrane by linking the UDP-Mur-NAc- pentapeptide to the transport lipid, called undecaprenyl pyrophosphate. Lipid II is produced when GlcNAc from UDP-GlcNAc is added to the lipid I. The pentapeptide cross bridges are added to the third amino

acid of the lipid II. Then, lipid II is transferred to the external side of the cell membrane by a protein assistant. Moreover, it is incorporated into nascent peptidoglycan by penicillin-binding proteins (PBPs). Lastly, PBPs catalysis reactions such as transglycosylation and transpetidation that lead to the glycan polymerization (Pinho M.G, *et al*., 2013).

Knowing the information above, it is interesting to discover more about this system and restoring susceptibility to strains that are resistant to antimicrobials. VraSR regulates the expression of more than 40 genes in *S. aureus* (Kuroda M, 2003), which are associated with peptidoglycan biosynthesis in response to cell wall inhibitors (Fan X, *et al*, 2007). Some of these genes, *murz*, *pbpb2*, *sgtb*, and *fmtA* and so many others, are clearly under the direct control of the VraSR system in the presence of oxacillin, vancomycin, and other cell-wall inhibitors (Sengupta M, *et al*., 2012). It has been demonstrated that *murZ* encodes Uridine diphospohate *N*-acetylglucosamine-1 carboxylvinyl transferase 2; *pbpB* encodes penicillin-binding protein *(PBP)* 2; *sgtB* encodes a putative monofunctional glucosyltransferase; and FmtA, which is an autolysis-methicillin-resistance protein, is encoded by *fmtA gene* (Utaida S, *et. al*., 2003).

1.3.2 Cell-wall associated genes regulation under *vraSR* promoter

As it has been confirmed at Dr. Sengupta Laboratory (2012), several genes, which are associated in cell wall biosynthesis, are under the *vraSR* regulatory mechanism. Understanding their functions could help us to identify any possible connections with the *vraSR* regulatory system.

The SgtB or MGT roles are important in terms of cell-wall stress conditions, especially in the final stage of peptidoglycan biosynthesis (Sengupta M, *et al*., 2012). Two types of enzymes are required to assemble peptidoglycan polymers: peptidoglycan glycosyltransferases (PGTs) and transpeptidase (TPs). *S. aureus* comprises two monofunctional PGTs such as SgtA and SgtB and one bifunctional PGT (PBP2), (Rebets Y, *et al.,* 2014). In the absence of PBP2, SgtB is more important than SgtA as it can replace transglycolase activity of PBP2. As a result, SgtB is essential in *S. aureus* viability (Reed P, *et al.,* 2011).

PBP2, the MRSA native protein, contains an N-terminal PTG domain and a C-terminal TP domain that accelerate carbohydrate chains cross-linking in cell wall biosynthesis (Pinho M, *et al.* 2001, Rebets Y, *et al*., 2014) According to Boyle-Varvra S. (2003), *pbp2* transcript levels increases by oxacillin and vancomycin inductions. Thus, the *pbp2* expression level could be upregulated by the VraSR (Gardete S, *et al*., 2006).

FmtA, a member of the VraSR regulon, is a low-affinity penicillin-binding protein contributing to peptidoglycan biosynthesis under cell wall stress in *S. aureus*. Active *fmtA* increases the level of peptidoglycan cross-linking (Zhao Y, *et al*., 2012). The *fmtA* gene was shown to be upregulated by cell wall-antibiotic stress (Sengupta M, *et al*., 2012). Accordingly, studies indicate that the VraSR system plays a critical role in preserving the "integrity" of the cell wall peptidoglycan and modulating the *S. aureus* response to cell wall damage, quite similar to an antibiotic resistance mechanism (Belcheva A, & Golemi-Kotra D, 2008).

1.3.3 VraS, the histidine kinase

HKs normally are membrane bound proteins that contain an N-terminal transmembrane sensing domain and a cytoplasmic C-terminal domain known as kinase core. The specific structural features of the HK family consist of a dimerization domain (DHp) and an ATP/ADP- binding or catalytic domain (Casino P, *et al*., 2010). Members of the HK family vary in size from <40 kDa to >200 kDa; the largest HKs are composed of five or six unique domains. *vraS* is a vancomycin-resistance-associated gene with homology to the histidine kinase family (Kuroda et al., 2000), located immediately upstream of *vraR*, a response-regulator homologue (Utaida S, *et al*., 2003). Analysis of the VraS amino acid sequence indicates that this typical HK protein is composed of an N-terminal transmembrane domain and a C-terminal conserved HK core (Belcheva A., & Golemi-Kotra, D, 2008). The N-terminal transmembrane domain of VraS consists of two membrane areas that are connected through a periplasmic connector. The conserved HK core of VraS contains the dimerization and histidine phosphotransfer (DHp) domain, which includes the conserved His residue, and the catalytic (CA) or ATP-binding domain (Gross R, 2012), (Figure 1.5).

1.3.4 Structural characteristics of VraR response regulator

A prototypical response regulator contains an N-terminal receiver (REC) domain connected to a variable effector domain by a flexible linker (Stock AM. *et al*., 2009). N-terminal domains have highly homologous structures consisting of an α-β construction with a central five-stranded parallel β-sheet surrounded by five α-helices. β-strands and the α-helices are connected by the loops arranged around the active-site aspartic acid that is

located at the end or top of the protein. Normally, the active site is composed of three Asp residues; the phosphorylatable Asp at the end of strand β3; and two Asp residues (or a Glu sometimes) are bordering the β1-α1 loop. The last two mentioned residues help to form an Asp-binding pocket that accepts a divalent metal ion prior to phosphorylation. (Bobay B.G *et.al.,* 2012).

In fact, most RRs are known as transcription regulators and are categorized into three sub-families based on their effector (REC) domain homology: the OmpR/PhoB winged helix binding domain, "the NarL/FixJ four-helix bundle domain, and the NtrC-ATPase-coupled transcription factors" (Robinson V.L, *et al*., 2000). According to the homologous RR NarL, VraR is a typical response regulator protein that has two domains composed of a conserved N-terminal receiver domain (REC) and a C-terminal DNA-binding or effector domain (ED) (Figure 1.5). The REC domain possesses a distinctive $(\alpha\beta)_5$ fold and is 117 bp in length (Liu Y, *et al*., 2009). The VraR effector domain has a four-helix structure that individually has a specific role in the VraR mediated genetic regulation. H1 (H7) is involved in activation, H2 (H8) is related to scaffolding, H3 (H9) aids in the DNA recognition, and H4 (H10) is involved in dimerization process (Donaldson L.W, 2008).

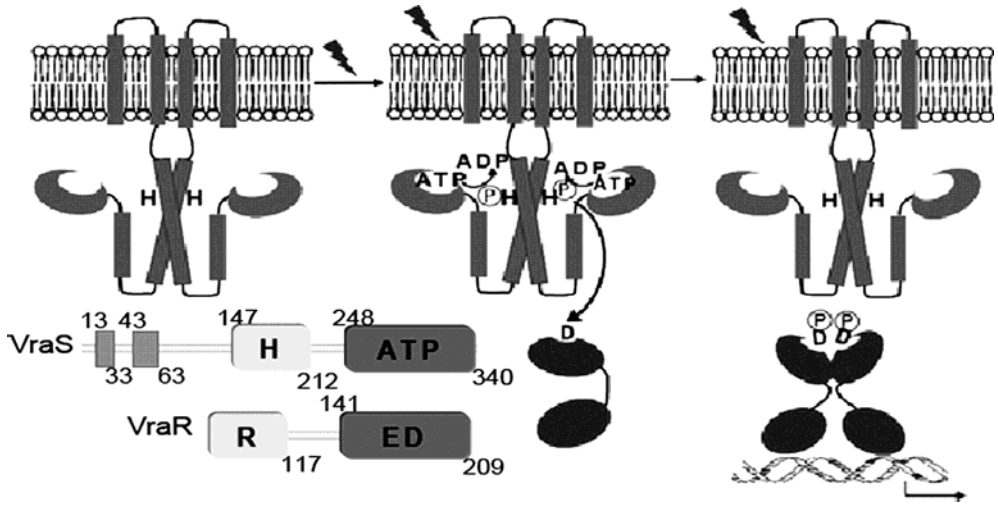

Figure 1. 5 The schematic demonstration of VraSR two component system is taken from Belcheva A., & Golemi-Kotra D. (2008)
The sensor HK, VraS and the response regulaor, VraR are shown with their amino acid positions on their domains. Phosphorelay process is also shown, starting from VraS autophosphorylation and transferring to the VraR and ending up to the VraR dimerization and DNA binding.H: histidine box; ATP: ATP binding domain; R: REC domain; ED: effector domain

1.3.5 VraSR signal transduction pathway

Both prokaryotic and eukaryotic HKs contain the same basic signaling components, namely a diverse sensing domain and a highly conserved kinase core that has a unique fold (Jung K, *et al.,* 2012). HKs undergo autophosphorylation in kinase core. Stimuli in different reconstituted full-length HKs can either enhance or inhibit kinase activities. To facilitate the understanding of HK regulation *in vivo*, additional methods are performed using ^{32}P labeling or a specific phosphate binding tag. As well as kinase activity, many HKs have phosphatase activity toward their cognate phosphorylated RRs. The DHp domain possesses the phosphatase activity that is due to the dimerization and catalytic domain interactions. As the RR phosphorylation level eventually determines the TCS pathways' output response, the

balanced regulation between the kinase and phosphatase activities of the HKs leads to the signal-induced adjustment of RR phosphorylation (Gao R, & Stock A.M, 2009). The RR-P dephosphorylation is not only the reversed RR-phosphorylation since it is not absolutely dependent on the HK. The phosphorylation and dephosphorylation are catalyzed by both HK and RR. Both of these proteins contribute in to the formation of an active site that facilitates the processes. In the case of phosphorylation, structural studies carried out with the HK839-RR-468 complex, show that the phosphor-acceptor Asp residue of RR is aligned with the phosphor-donor His residue of HK, favoring phosphoryl group transfer reactions. This alignment is facilitated by binding of the RR to the helical stem of one HK subunit through interactions of helix-α1 of DHp domain with the first helix and the last loop of RR (Casino P, *et al*., 2009). In the case of dephosphorylation, a water molecule is needed to be activated by His residue of DHp in order to attack the phosphorus atom of the Asp-P species. However, structural studies show that the HK-RR complex discussed above forms active site that supports the dephosphorylation mechanism (Casino P, *et al*., 2010).

The signal transduction pathway by VraSR is proposed to happen as follows. Upon cell wall damage, VraS monitors extracellular stimuli and modulates the activities by sending input signals to the sensing domain. Recent studies on YvqF (VraT) shed new light on the VraSR regulatory system process, which is shown in VISA-clinical isolates, and appears to detect cell-wall damage. It is a transmembrane protein and is located immediately upstream of *vraS.* The *S. aureus* YvqF demonstrates amino acid similarity to *B. subtilis*-LiaF, acting as an inhibitory element on LiaR expression, which is also VraR orthologous

(Boyle-Varvara S., *et al*., 2012).

The phosphorylation process is initiated by transferring a phosphoryl group from ATP to a conserved His residue of the VraS. Subsequently, the phosphoryl group is transferred from the phospho-His residue to a conserved Asp-55 of VraR while being catalyzed by the regulatory domain. Finally, the phosphoryl group is transferred from the phospho-Asp residue to a water molecule via a hydrolysis reaction (Stock A.M, 2009; Laub M.T, 2011). The phosphotransfer reaction showed that this event is faster than VraS autophosphorylation *in vitro*; and about 70% of the VraR phosphorylation is happening within 30 seconds. This result, along with the fast kinetics of VraS autophosphorylation, proposed that the VraSR complex could contribute in transducing cell wall stress *in vivo* rapidly (Belcheva A, & Golemi-Kotra D, 2008).

Asp-55 phosphorylation also builds a conformation in the VraR REC domain and stimulates its dimerization by dislocating the inter-domain interface to form a dimer on the DNA-binding domain. X-ray crystal structure analysis reveals a considerable remodeling of the REC domain, creating a deep hydrophobic surface known as a "hydrophobic pocket." The hydrophobic surface is positioned between α_1 and α_5 helices and is responsible for VraR dimerization. During VraR dimerization, Metionine-13 (M13) residue docks into this "pocket." Correspondingly, an M13 mutation to Glutamic acid (D) prevents VraR from forming the dimer without any significant changes on the overall fold and catalytic activity (Leonard P.G, *et al*., 2013). This fact showed the importance of this residue in VraR dimerization. In the active VraR structure Thr83 and Tyr102, known as the switch residues,

adopt a distinctive active conformation, with the –OH- group of Thr83 and the phenol ring of Tyr102 establishing direct hydrogen bonds with beryllofluoride and the backbone carbonyl of Phe85.

1.3.6 VraR DNA binding activity

The VraR DNA-binding domain consists of four α-helixes (Leu148 to Gln209). The H2 (H8) and H3 (H9) form a classical helix-turn-helix (HTH) (Donaldson L.W, 2008). HTH is a fundamental structural motif containing two α-helixes connected by a short strand of amino acid that exists in proteins and can bind to DNA. Ultimately the HTH forms dimers in the active VraR protein after phosphorylation process. Then, VraR binds to specific regions of the VraSR promoter (PVraSR). According to the previous predictions, helix H9 (residues Ile176 to Leu190) is the DNA-recognition that slots into the DNA major groove (Liu Y.H, *et al*., 2009). Nevertheless, the DNA binding site of VraR-P is the H8–turn–H9 motif in the C-terminal domain. The DNA binding domains create dimers in the active VraR protein, and the hydrophobic face of α10 is burying certain protein surface area with the C-terminal end of α7 in the dimerization interface (Leonard P.G, *et al*., 2013).

The DNase I footprinting analysis indicates that VraR binds to three distinct sites which are located on positions -76 (R3), -60 (R1) and -35 (R2) depending on its phosphorylation state (Belcheva A, *et al*., 2009). R1 is demonstrated to be a phosphorylation independent and high-affinity binding site, which serves as a means of recruitment of VraR to its promoter under normal growth conditions and gene expression regulation. On the other hand, R2 is known as low-affinity and phosphorylation-dependent site, which gets occupied

by phosphorylated VraR (VraR-P) under cell wall antibiotic stress as a result of VraSR operon upregulation (Belcheva A., *et al*., 2011).

1.3.7 *vraR* mutants in VISA strains

Recently it has been proposed that genetic alterations in TCS genes such as *vraSR*, *graSR*, etc., have an effective influence on glycopeptide-resistance phenotype (Kuroda M, *et al*., 2003; Meehl *et al*., 2007; Neoh *et al*., 2008). Another study also demonstrated that the evolution of VISA from VSSA strains during "persistent infection" related to the failed vancomycin treatment, could be due to a single base substitution (Kato Y, *et al*., 2010). Accordingly, the first study on the point mutations between clinical VISA and VSSA, and their amino acid changes has commenced. In this research, sequences of *vraSR*, *graSR* and many more were investigated from VISA and VSSA strains collected from hospitals. The analysis of the prevalence of amino acid substitutions in the VraR such as, E59D, A113V and S164P, demonstrated that the corresponding mutations in *vraR* were associated with the emergence of a VISA strain from the VSSA strain after constant exposure to vancomycin. The occurrence of the above amino acid changes was different in VISA and VSSA strains. Although the prevalence of mutations in *vraR* of VSSA strains was lower than that of VISAs, the number of VISA strains bearing mutations (including positions other than those above) was high compared with the number of VSSA respectively. Furthermore, the above mutations were demonstrated to be involved in glycopeptide resistance in VISA (Yoo J.I, *et al*., 2013). As a matter of fact, our primary lab interest was to study VraR variants in the signal transduction pathway by VraSR.

2 CHAPTER TWO: IN VITRO AND IN VIVO INVESTIGATION OF VraR MUTATION ON ITS REPONSE TO CELL WALL DAMAGE

2.1 Introduction

The main aspect of this research is to focus on VraR protein as on of the major targets for antibiotic resistant mechanism (Gao R, & Stock A.M, 2009). As it has been reported that TCRS gene alterations contribute to the glycopeptide-resistance phenotype like in the *vraSR* genes (Yoo J.I, *et al*., 2013), various point mutations, in either clinical or lab strains were tested. We decided to examine the point mutations in *vraR* that lead to the following amino acid substitutions, E59D, S164P, and A113V, which were identified in the clinical strains due to their strong relationship with the glycopeptide resistance (vancomycin). Moreover, S164A and M13A from previous studies are also chosen to study (Figure 2.1). S164A, adopted from S164P was used to analyze the difference of single point mutation from proline to alanine and possible changes that may occur. Also, Methionine-13 (Met-13) positioned on the α1-helix of VraR, which was shown by crystallography to be involved in dimerization of VraR upon phosphorylation (Stock A.M, 2013), is tested for the potential consequences. Initially, the phosphorylation and dimerization ability of VraR mutants were examined in order to compare with the VraR wild type. This was followed by analysis of protein-DNA interactions and possible effects of Oxacillin on VraR regulon genes such as *fmtA, pbp2, and sgtb in vivo*. Understanding the VraR signal transduction pathway is important in order to know this protein functions in the stress conditions. If we can comprehend its structural transitions and how the signal is

disseminated to the DNA binding domain, we can design pharmaceuticals to eliminate antibiotic resistance progression by targeting VraR protein.

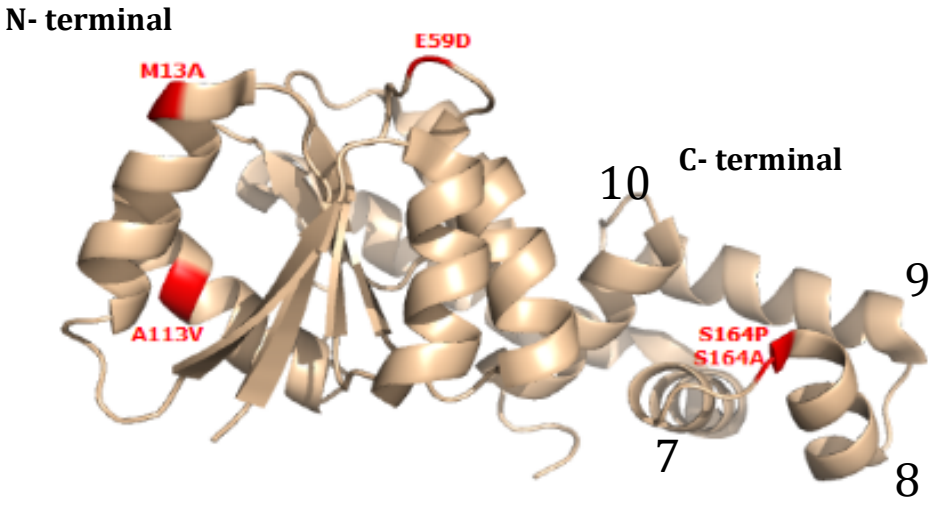

Figure 2. 1 The schematic presentation of VraR and amino acid substitutes location
M13, E59, and A113 (in red) are located at the N-terminal domain and S164 (in red) is located at the C-terminal domain (Numbers at the C-terminal domain are representing the number of alpha-helixes).

2.2 Materials and Methods

2.2.1 Chemicals

Chemicals, growth media, and antibiotics were purchased from Thermo-Fisher (Whitby, Canada) or Sigma (Oakville, Canada), unless otherwise stated. *Escherichia coli* strains, Nova-Blue and BL21 (DE3), and other expression plasmids were purchased from EMD4 Biosciences (New Jersey, USA). All the primers were purchased from Sigma (Oakville, Canada). Chromatography columns and media were bought from GE-Healthcare (Mississauga, ON, CA). Radioactive [γ-^{32}P]-ATP was purchased from Perkin Elmer (Life and Analytical Sciences, Waltham, MA, USA).

2.2.2 Generation of VraR and its variants

The *vraR* and its variants (VraR M13A, VraR S164P, VraR S164A, and A113V) were cloned into the pET26b vector and transformed into *E. coli* BL21 (DE3) by other co-workers in Dr. Golemi-Kotra's Lab. The Glu-59 residue of VraR (encoded by GAA) was mutated to Asp (encoded by GAC) by performing a mutagenic polymerase chain reaction (PCR) using *pfu* Turbo™ DNA polymerase, and the designed primers (Table 2.1). To digest only the methylated template DNA (pET26b::VraR) construct , *DpnI* endonuclease digestion was done on the PCR product, and the resulting mixture was used to transform *E.coli* NovaBlue competent cells. At the end, the final construct was transformed into *E.coli* BL21 (DE3). The Centre for Applied genomics (TCAG) facilities (Sick Kid's Hospital) confirmed the mutation of the E59D by performing DNA sequencing

analysis (Raw sequencing data are in Appendix A, Figure A1).

Table 2. 1 primers designed to generate VraR E59D mutant. Italic bases represent the mutated codon.	
Primer Name	**Primer Sequence (5'-3')**
VraR E59D FW	**GATTTACTTATG*GAC*GACATGGATGGTG**
VraR E59D Rev	**CACCATCCATGTC*GTC*CATAAGTAAATC**

2.2.3 Production and purification of wild type/Mutant proteins

VraR wild type, its variants and VraS protein purification were carried out as described by Anthoneta Belcheva (2008).

2.2.4 Circular Dichroism (CD) spectroscopy and Thermal melting of VraR

CD measurement of the target protein was carried out by preparing a protein solution of 10 μM in an equilibration buffer (20mM Tris, 5mM $MgCl_2$, pH 7.0). The CD spectrum was recorded from 200 to 260 nm using a Jasco J-810 instrument (0.1 cm path length cuvette). To investigate the effect of the mutation in the overall structure of

the protein, the thermal melting process of the protein was carried out by monitoring the effect at 222 nm between 20°C-100°C using the Jasco J-810 instrument.

2.2.5 Phosphorylation of VraR by Lithium potassium acetyl phosphate

Protein solutions of VraR at 10 µM and 20 µM in the phosphorylation buffer (1XPB 50 mM Tris, 50 mM KCL, 20 mM $MgCl_2$, 4 °C, pH 7.4) were supplemented by 50 mM acetyl phosphate and incubated for 1h at 37 °C to facilitate phosphorylation of VraR or its variants. The sample could be tested for Phos-tag™ gel and Native-PAGE gel electrophoresis for the following purposes.

2.2.5.1 Phos-tagTM gel electrophoresis

Quantification of VraR phosphorylation was investigated using SDS-PAGE supplemented with a Phos-tag™ affinity chemical. The gel consist of a separating gel containing 10% Acrylamide, Tris-Cl, pH 8.8, 10% SDS, 10% APS, 100 mM $MnCl_2$, TEMED and 20mM phos-tag, and the same stacking gel as SDS gel. SDS stacking gel is composed of 30% Acrylamide, Tris-HCl 0.5mM pH 8.8, 10% SDS, 10% APS, TEMED, dd-H_2O. Phosphorylation quantification was done by Image-J software.

2.2.5.2 Native- PAGE gel electrophoresis

Dimerization abilities of VraR and its variants upon phosphorylation were examined by Native-PAGE. Proteins with different concentrations of 10 µM, 20 µM, and 30 µM were phosphorylated by 50 mM acetyl phosphate, and were loaded on 10% Native gel at 4°C after 1h incubation (37°C). Native-PAGE gel is the same as SDS gel but lacks SDS. SDS-PAGE gel consists of a separating and a stacking gel (shown at the

phos-tag™ section) that in separating gel, 1.5mM Tris-HCL is used. Native running buffer contains 25 mM Tris and 192 mM Glycine was used to run the gel with.

2.2.6 In vitro phosphorylation of VraR by VraS-P

VraS (20 µM) phosphorylation was started by radioactive ATP (ϒ-^{32}P, 3000Ci/mmol) and phosphorylation buffer (1XPB: 50 mM Tris, 50 mM KCl, 5 mM $MgCl_2$, 10 mM $CaCl_2$), and followed by VraR phosphorylation. The unreacted ATP was removed, by using Zeba desalting column after 1 h incubation (RT), and mixed with 20 µM VraR in a time order. Quenching the reaction with SDS-loading dye (250mM Tris-Cl, pH6.8, 8% SDS, 0.1% Bromophenol blue, 40% glycerol) was done in time intervals for 0, 0.5, 1,3,5,7,and 10min. For analyzing, 15% SDS gel was used, and then it was visualized by exposing it the gel to phosphor screen plus Typhoon Trio instrument (GE-Healthcare).

2.2.7 DNase-I footprinting assay

To perform this assay, *vraSR* promoter (P_{VraSR}) between -121 to +26 was amplified by PCR using the following primers:

Dir: 5' ACGAAGCTTGGTCCGATTTTAACGACAAAAATTG-3' and

Rev: 5'-TGAAATGACGCATTGATTGTGTTC-3'. Then, the primer of interest (direct primer in this case) was 5'-end labeled with T4 polynucleotide kinase (NEB) in the presence of ATP (ϒ-32P, 3000Ci/mmol), and then it was re-amplified by PCR. The following PCR conditions were used: 95 °C for 5 min, 30 cycles of 95 °C for 30 s, 62 °C for 30 s, 72 °C for 30 s, and a final extension step at 72 °C for 5 min. Target^{32}P-labeled promoter was purified by QIAquick Gel Extraction Kit (Qiagen) to use as a template with

different VraR/VraR-P concentrations (0, 2, 5, 25, and 50 µM) and added to the binding reaction mixture (10X Binding buffer: 100 mM Tris pH 7.5, 500 mM KCL, 10 mM DTT, supplemented with 10 mM $MgCl_2$, 50% Glycerol, 20 ng/µl Herring sperm DNA). The binding reactions were subjected to DNase-I for 2min and then the DNase I stop solution (1% SDS, 0.2 M NaCl, 20 mM EDTA, pH 8.0) to digest the DNA. Protein was extracted by addition of 1:1 Phenol:Chloroform and precipitated by ethanol. The pellets having the DNA were air dried, and resuspended in 10mM formamide, 1mg/ml bromophenol blue, and 1mg/ml xylen cyanol, called loading dye. Then it was analyzed by loading samples on 8% polyacrylamide gel containing urea, and after exposing it to phosphor screen it was visualized by Typhoon Trio^{+} Variable Mode Imager (GE-HealthCare).

2.2.8 Construction of the pMK4::*vraR*::P*vraSR* $_{(-121 \text{ to } +150)}$ plasmid complementing vector

Previously, P*VraSR*$_{-462 \text{ to } +150}$ variants were constructed by fusing the promoter upstream of the *lux* operon reporter vector pXEN1 (Belcheva A. *et al*., 2009) and it was demonstrated that in the presence of Oxacillin the luminescence signal increased by ~60-fold for P VraSR::lux. Therefore, we decided to choose a segment of the above region from -121 to +150 with respect to the transcription start site to perform the *in vivo* studies.

To perform *in vivo* studies by RT-qPCR and comparing the VraR regulon genes expression in different *vraR* variants, the promoter region of *vraSR* (P_{vraSR}), spanning between -121 to +150 was ligated to the *vraR* gene and cloned into the pMK-4 vector between *EcoRI* and *SalI* restriction sites after their extraction independently. For this

purpose, the desired regions of the promoter and the *vraR* gene were amplified using designed primers (Table 2.2), and 2.5 U *pfu* Turbo^{TM} DNA polymerase by PCR conditions as follow: 95 °C for 5 min, 30 cycles of 95 °C for 30 s, 52 °C for 30 s, 72 °C for 1min, and a final extension step at 72 °C for 10 min. Both products were gel purified from 1% agarose gel by QIAquick® Gel extraction kit (QIAgen) and digested with *BamHI* and ligated to each other. The resulting product was amplified using similar PCR conditions and after gel purification it was mixed with equal volumes of End conversion buffer at 22 °C for 15 min, that was provided with the pSTBlue-1 vector (Perfectly Blunt ® Cloning Kit, EMD Millipore). Then, it was mixed by T4 DNA ligase (NEB) at 25 °C for 1h. Afterwards, the plasmid was transformed into NovaBlue competent cells by heat shock (42 °C, 1min) and were grown on X-Gal LB agar supplemented by 50 μg/ml Kanamycin and 80 μM IPTG to discriminate between recombinant (white colonies) and non-recombinant cells (blue colonies). The pSTBlue-1 extraction was done as mentioned above, and the confirmed desired insert was ligated to the pMK-4 vector (following the gen : plasmid ratio: 3:1) between *EcoRI* and *SalI* restriction sites. Finally the plasmid was transformed into NovaBlue cells by heat shock. Successful cloning and transformation was confirmed by DNA sequencing (TCAG facilities). The already confirmed isolated plasmid from NovaBlue was introduced to *S.aureus* RN4220::Δ*vraR* competent cells by electroporation (2 kV, 2.5 ms) using Micropulser (Bio-Rad) and were grown on TSB agar supplemented by 10 μg/ml chloramphenicol. Glycerol stock of the chosen colonies after plasmid digestion were prepared and kept at -80 for further investigations.

2.2.8.1 Single-site mutation of pMK4 containing *vraR* and its promoter

The already mentioned constructed plasmid was extracted for the single-site mutation to generate the *vraR* mutants (VraR M13A, E59D, S164P, and S164A). Primers containing targeted mutations were used to PCR-amplify pMK4 containing *vraSR* promoter region and *vraR* gene (Table 2.2). The PCR-mutagenesis was performed as follow including a "hot start (95°C)" and a "heated lid:on": 95 °C for 1 min, 16 cycles of 95 °C for 30 s, 55 °C for 1 min, 68 °C for 10 min and a final extension step at 68 °C for 10 min. The products were digested by DpnI and then transformed into NovaBlue competent cells by heat shock. After growing cells on LB plates containing 50 µg/ml kanamycin, mutations were confirmed by plasmid sequencing (TCAG facilities). Plasmids containing the anticipated mutation were transformed into RN4220*ΔvraR* competent cells by electroporation and spread on Tryptic Soy Broth (TSB) agar supplemented by 10 µg/ml Chloramphenicol. Glycerol stocks of the confirmed transformation were prepared and kept at -80 for further investigations.

2.2.9 RNA isolation from *S. aureus* RN4220

Overnight seed cultures of each RN4220 cells were prepared in TSB media supplemented by 10 µg/ml chloramphenicol. 160 µl of overnight seed cultures were used to inoculate 16 ml TSB medium supplemented with 10 µg/ml Chloramphenicol and incubated at 37°C (200 rpm) to achieve OD_{600}: 0.4. The cultures were split into two 5-ml in a 15ml sterile tube and one was treated with 10 µg/ml oxacillin which was incubated along with the control tube –non oxacillin treated tube- at 37 °C for 30 min. 1ml of each tube were mixed thoroughly with 2 ml of RNA Bacteria Reagent (Qiagen) for 10 s and incubated 5 min at

room temperature (RT) and then centrifuged at 7700rpm for 15min. The resulted pellets were resuspended into 180µl TE buffer (30 mM Tris, 1mM EDTA, pH 8.0) and 20 µl of 1.25 mg/ml lysostaphin following by 30 min incubation at RT. 1 µl proteinase K (NEB) was added, and the suspensions were incubated at RT for another 30 min. 700 µl of RLT buffer were added and the suspensions were vortexed for 15 s. 2-ml tubes containing 100 µl silica glass beads were prepared to transfer our samples in and vortexed 3 times for 20 s, and let them rest for 20 sec in between. The samples were spun for 1 min at 13000 rpm, and the supernatants were transferred into new tubes which then 470 µl of 100% ethanol were added. Each time 720 µl of the samples were loaded onto RNeasy Mini spin columns and centrifuged at 13000rpm for 30 s and then washing step was done by 350 µl of RW1 buffer and twice by 500 µl RPE buffer. Centrifugation was done for 1 min to eliminate excess ethanol and the total RNA was eluted by 50 µl Dnase-Rnase free water. 5 µg of the RNA were digested by 2 µl of DNase-I (2000U) for 20min at 37°C that inactivated afterward by 0.5 M EDTA for 10 min at 75°C.

Table 2. 2 primers designed to generate pMk4_VraSR.
VraR cloning and mutations in pMK4 containing the recent cloned segments. Italic underlined bases represent the restriction sites and mutations.

VraSR FW	**5'AG*GAATTC*GGTCCGATTTTAACGACAAAAATTG**	***EcoRI***
VraSR Rev	**5'CG*GGATCC*ACGTTCAACATAGTTCATAAC**	***BamHI***
VraR FW	**5'CG*GGATCC*ATG ACGATTAAAG TATTGTTTG**	***BamHI***
VraR Rev	**5'GC*GTCGAC*CTA TTG AAT TAA ATT ATG TTG**	***SalI***
S164A FW	**5'GATTGCGAAAGGTTAC*GCA*AATCAAGAAATTGCTAG**	**-**
S164A Rev	**5'CTAGCAATTTCTTGATTTG*CGT*AACCTTTCGCAATC**	-
M13A FW	**5'GTGGATGATCATGAA*GCG*GTACGTATAG**	-
M13A Rev	**5'CTATACGTAC*CGC*TTCATGATCATCCAC**	-
S164PFW	**5'GATTGCGAAAGGTTAC*CCA*AATCAAGAAATTGCTAG TGC**	**-**
S164P Rev	**5'GCACTAGCAATTTCTTGATT*TGG*GTAACCTTTCGCA ATC**	**-**
E59D FW	**5'GATTTACTTATG*GAC*GACATGGATGGTG**	-
E59D Rev	**5'CACCATCCATGTC*GTC*CATAAGTAAATC**	-

2.2.10 q-RT-PCR to investigate the level of VraR regulon genes in *S. aureus* RN4220 and its mutant strains

High Capacity RNA-to-cDNA kit (Life Technologies) was used to synthesize cDNA from 500ng of DNase-I treated RNA. 16sRNA gene was used as an internal control using designed primers: Dir 5'GCTAAGTGTTAGGGGGTTTCC and Rev 5'TTCAACCTTGCGGTCGTACT. The 20 µl reactions were prepared consisting of 25 ng of cDNA, 0.25 µM of each primer (accordingly designed to target specific gene, Table 2.3), and 10µl of SYBRE SELECT Master Mix (Life Technologies). PCR conditions were done by a Rotor-gene Q qRT-PCR cycler (Qiagen) as follows: First hold: 2 min at 50 °C, second hold:10 min for 95 °C, 40 cycles of 95 °C for 15 s, 60 °C for 30 s, and 72 °C for 30 min; and 72 °C for 10 min as a final extension step.

2.2.11 MIC of RN4220, ΔVraR and ΔVraR complemented wild type and mutant strains

A 96-well microliter plate with 200 µl culture volume was used to determine vancomycin Minimum Inhibitory Concentration (MIC). In the presence of pMK4 plasmid, 10 µg/ml chloramphenicol were added to the TSB media. Overnight seed cultures (450 µl) were grown in TSB (50 ml) at 37°C, 200 rpm and the OD_{600nm} was recorded and adjusted to 0.05. Cells were grown in 50 ml TSB at 37 °C to achieve the OD of approximately 0.5. At this step a serial dilutions were done to obtain the final inoculum concentration close to 5 x 10^5 CFU/ml. First, the suspension was diluted 1:10 in TSB and then this step was repeated to

get 100 folds dilution in total. Then, 100 µl of the final dilution were used to inoculate all the wells containing 2-fold of vancomycin. Plates were incubated at 37°C for 24 and 48h without any shaking and OD_{600nm} was measured by Synergy H4 plate reader (BioTek).

2.3 Results

2.3.1 Purification of VraR by FPLC

VraR wild type and mutants were purified using the DEAE- Sepharose and Heparin-Sepharose columns. Each protein was eluted from DEAE column around 20-30% of the linear gradient of the elution buffer (Figure 2.2a), and was eluted from the Heparin column around 55-60% (Figure 2.2b).

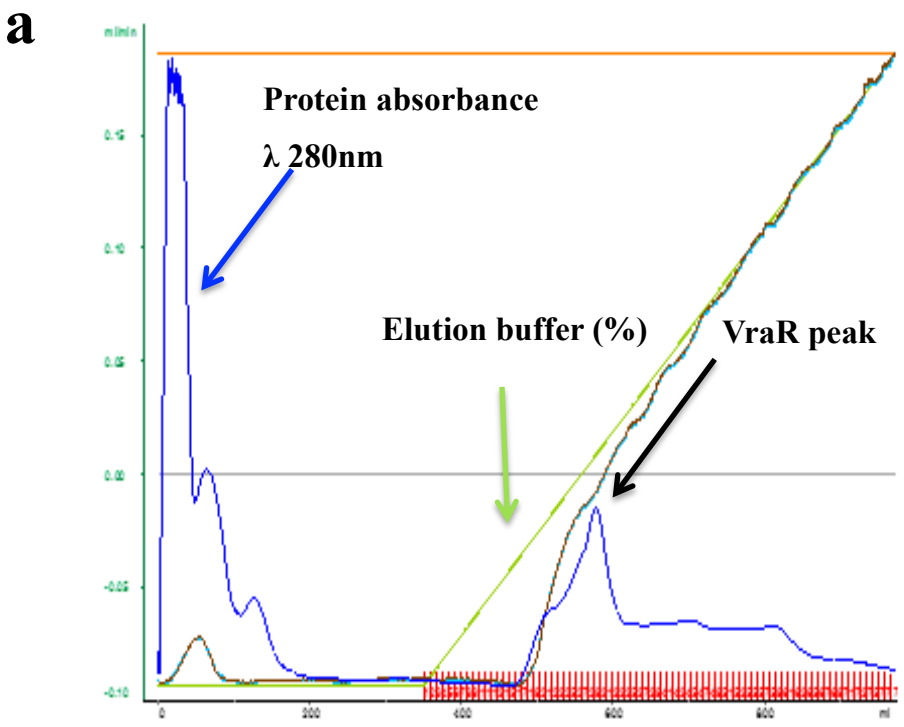

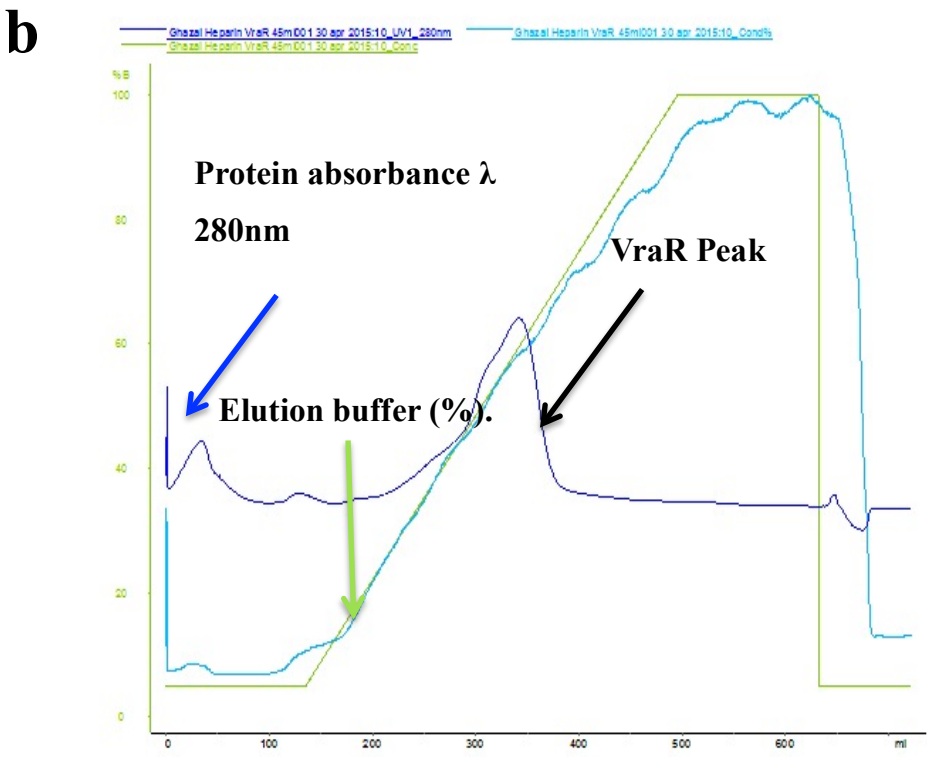

Figure 2. 2 FPLC UV (280nm)-chromatogram showing protein eluted from purification columns.
(a) FPLC UV (280nm)-chromatogram showing protein eluted from DEAE column. VraR wild type and mutants are eluted around 40-60% gradient of elution buffer (500mM Tris pH 7.0, and 5 mM $MgCl_2$). (b) Chromatogram showing protein eluted from Heparin column. VraR wild type and mutants are eluted around 40-60% gradient of elution buffer. Y axis: Elution buffer content (%); X axis: Order numbers of collection tubes; The blue and green lines are representing protein absorbance λ 280nm and content of elution buffer (%).

2.3.2 CD & thermal melting

CD technique was used to help us defining a protein structure-folding pattern. This method showed that a protein is correctly folded, miss-folded or denatured. According to

the circular dichroism spectra, VraR wild type and mutants showed similar CD patterns with large amount of beta-sheets. Therefore, by overlapping all the spectra, it was indicated that all proteins possessed identical secondary structures (Figure 2.3).

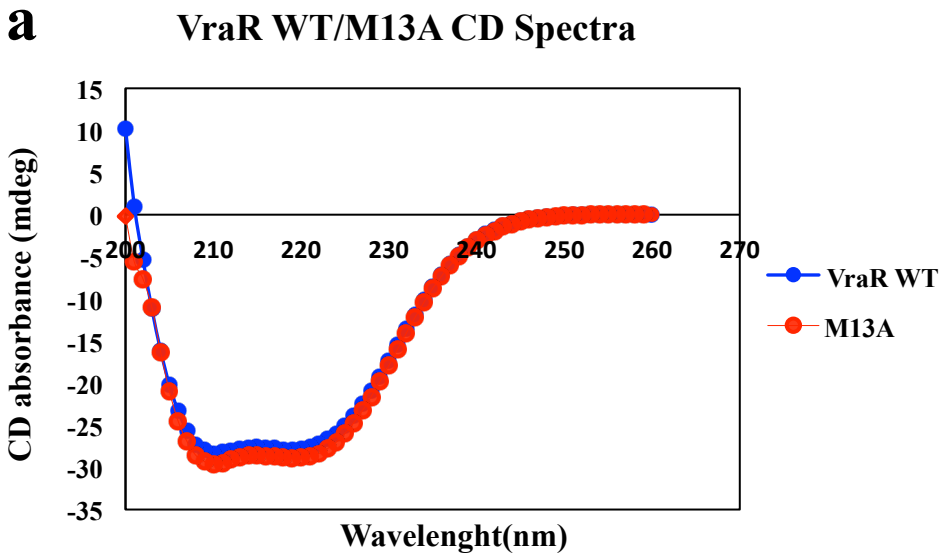

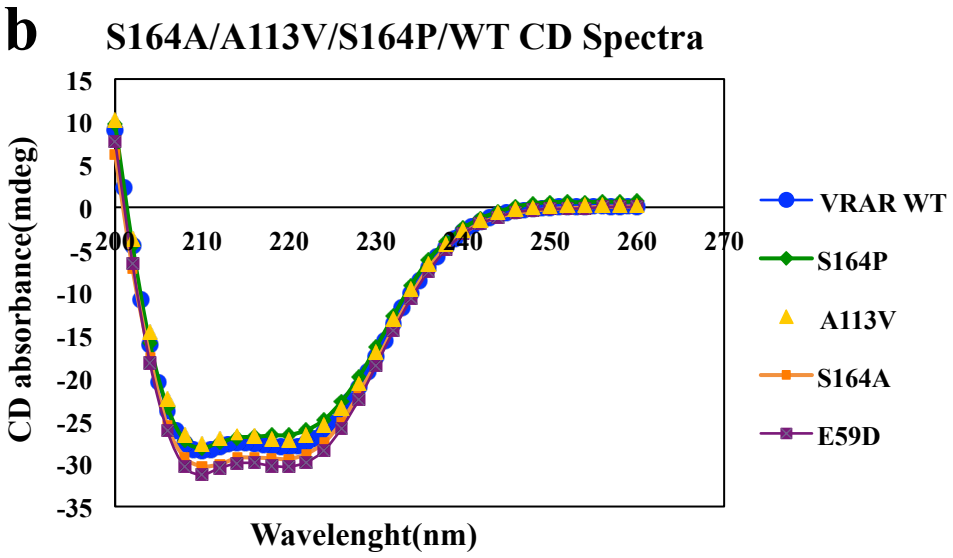

Figure 2. 3 Circular dichroism Spectra of VraR wild type and mutants (M13A, E59D, S164P, S164A, and A113V).
(a) VraR WT and M13A (10 µM) spectra in an equilibration buffer (20mM Tris, 5mM MgCl2, pH 7.0) was acquired at 22°C. (b) Spectra represents VraR WT and the rest of the mutants (S164P, A113V, S164A, and E59D).

Thermal melting was performed to provide more information about proteins potential stability and to compare the effects of mutation on them. For this purpose the temperature dependent protein denaturation was monitored using Circular Dichroism spectroscopy. Absorbance at 260nm was observed in different ranges of temperature and the Tm was estimated as measuring the middle point of the melting curve. In fact, the mutants showed the same melting point at around 50.5-60°C as wild type, which means mutation did not alter protein-native structure (Figure 2.4).

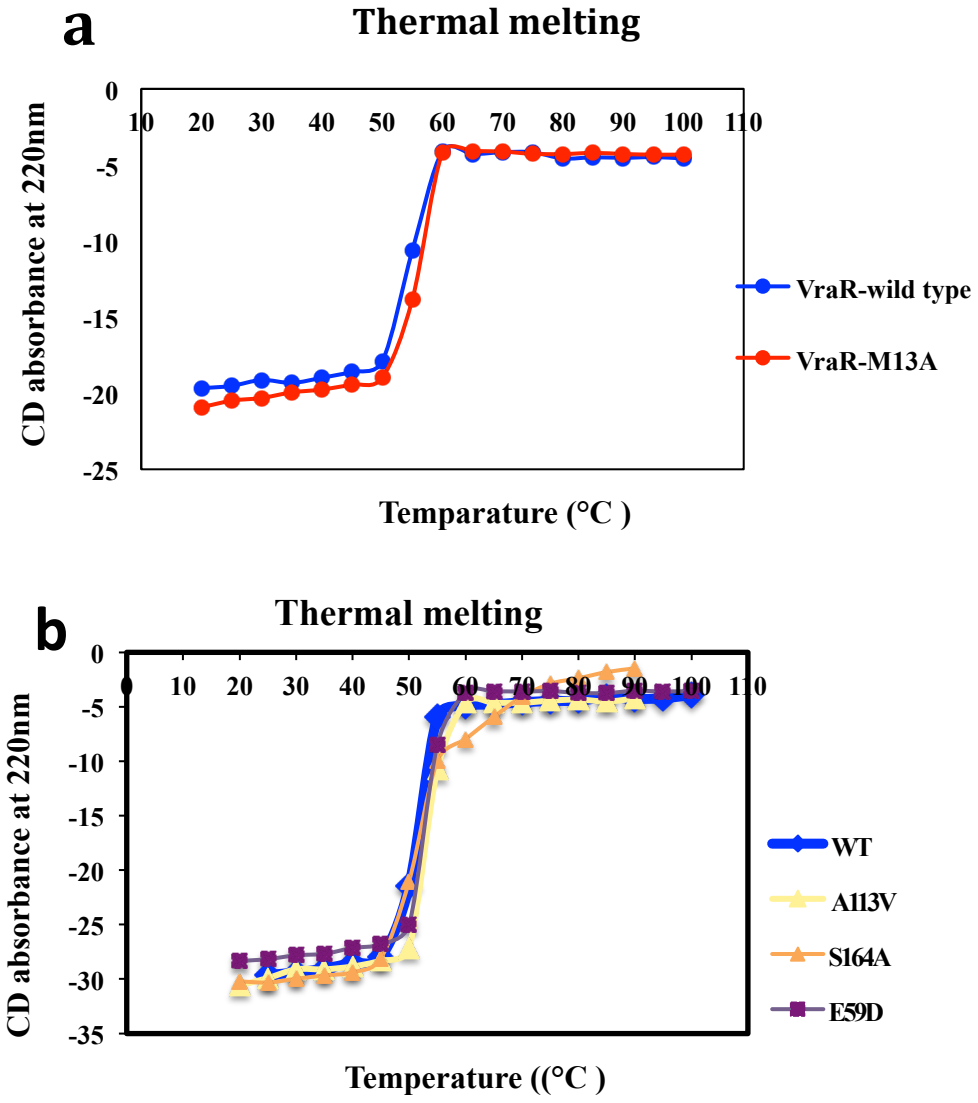

Figure 2. 4 Thermal melting analysis of VraR WT and mutants.
(a) Thermal melting curves of VraR WT and M13A (10 µM) were obtained by monitoring changes in flexibility at 222nm as temperature was increased at a rate of 2°C, in the range of 20°C -90°C. **(b)** Thermal melting curves of VraR WT, A113V, S164A, and E59D.

2.3.3 Analysis of protein phosphorylation by phos-tag™ gel electrophoresis

VraR proteins phosphorylation estimation was done by phos-tag™ gel electrophoresis. The results demonstrated that the wild type VraR has the ability to accept the phosphoryl group but Vra M13A underwent phosphorylation at a much lesser extent in comparison to other mutants (Figure 2.5). However, according to the quantification results from two or three different trials, VraR S164A phosphorylation rate is the highest one in comparison to the wild type and the rest of the mutants after 30 min (Figure 2.6).

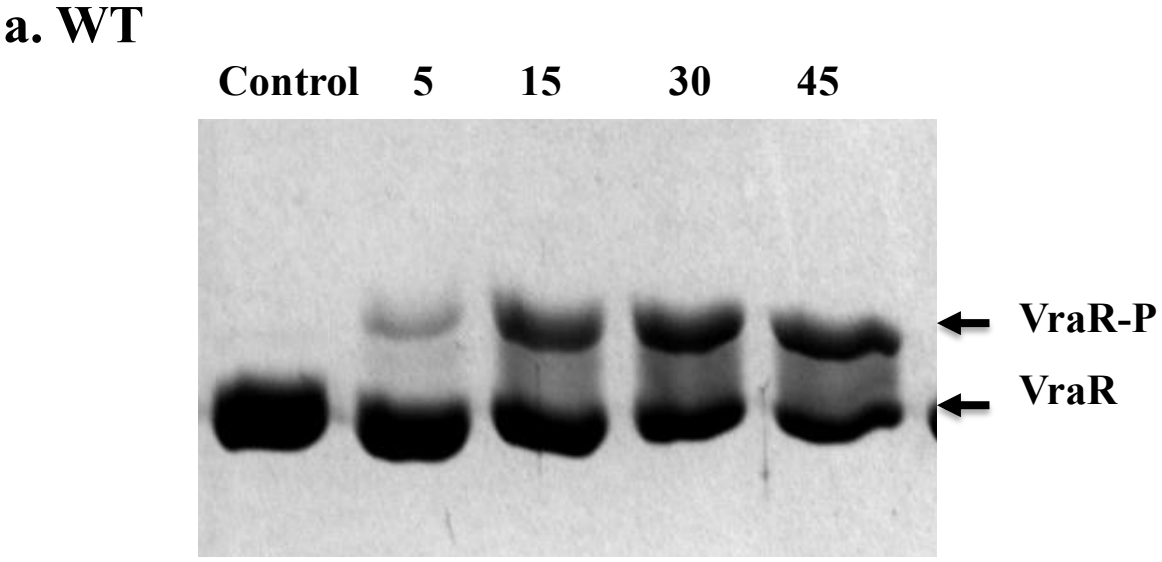

b.M13A

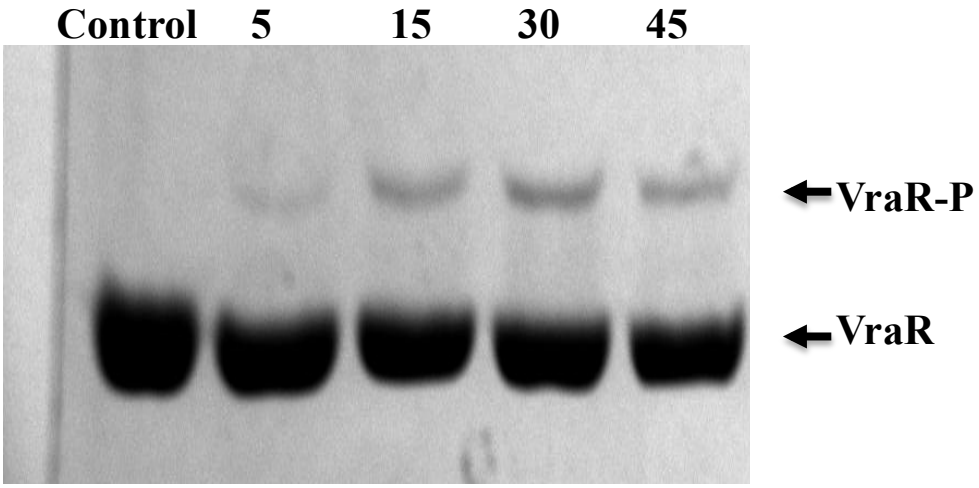

c. E59D

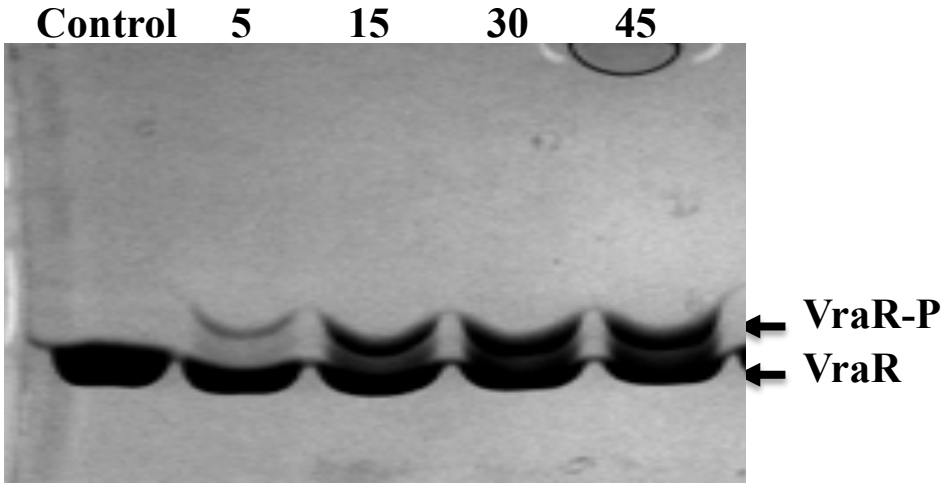

d. S164A

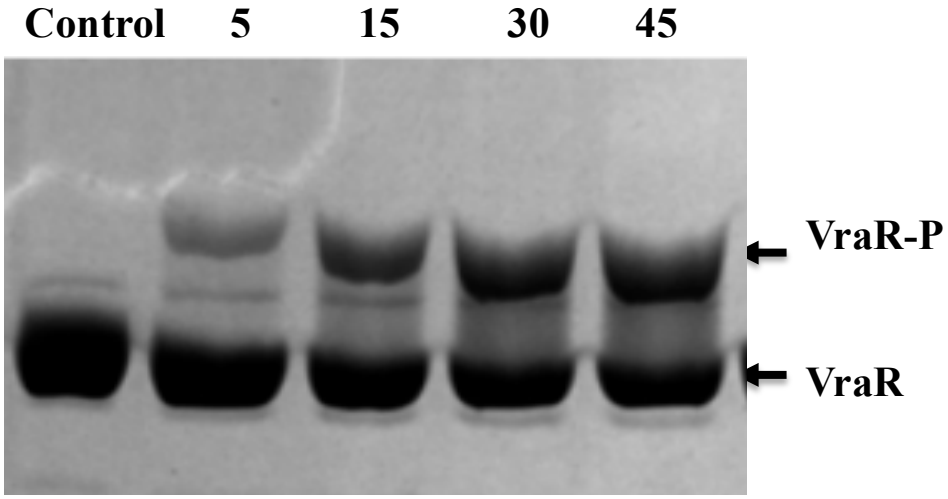

e. S164P

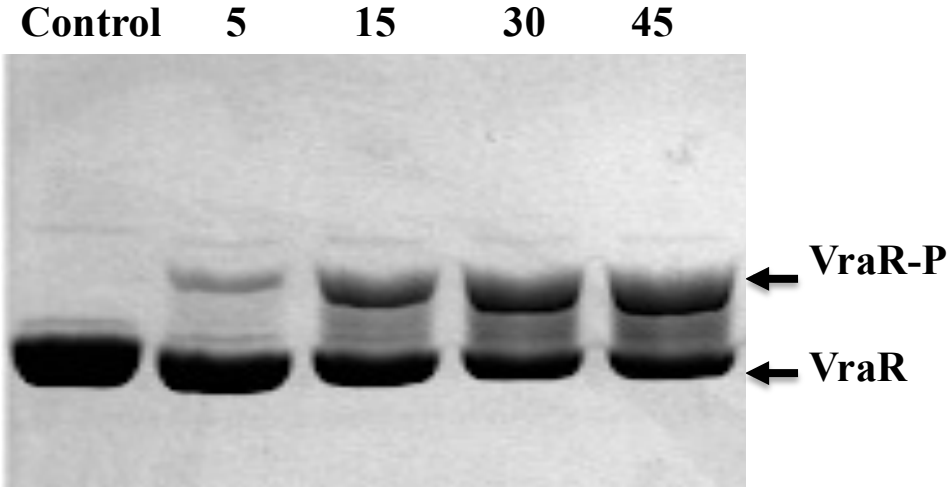

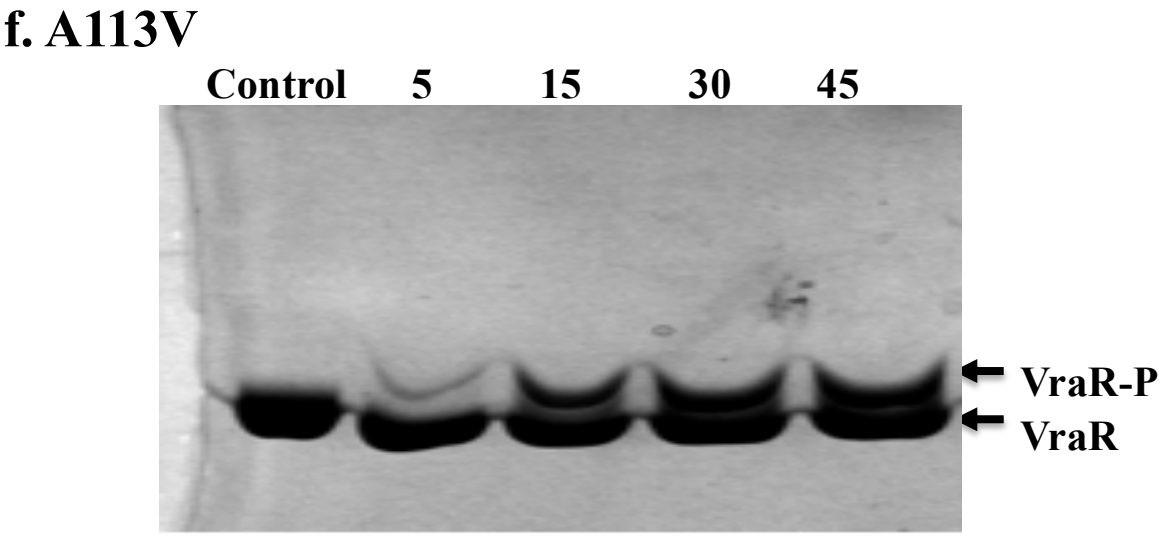

Figure 2. 5 Phosphorylation analysis of VraR wild type and mutants by Phos-tag gel. 20 μM VraR was phosphorylated by 50 mM Acetyl phosphate(AP) at 37°C and quenched by an SDS dye in time intervals and loaded on 12.5% SDS gel containing phos-tag and $MnCl_2$Lane 1: controls having no AP, Lane 2-5: quenching time intervals(a) VraR WT (b) VraR M13A (c) VraR E59D (d) VraRS164A (e) VraR S164P (f) VraR A113V

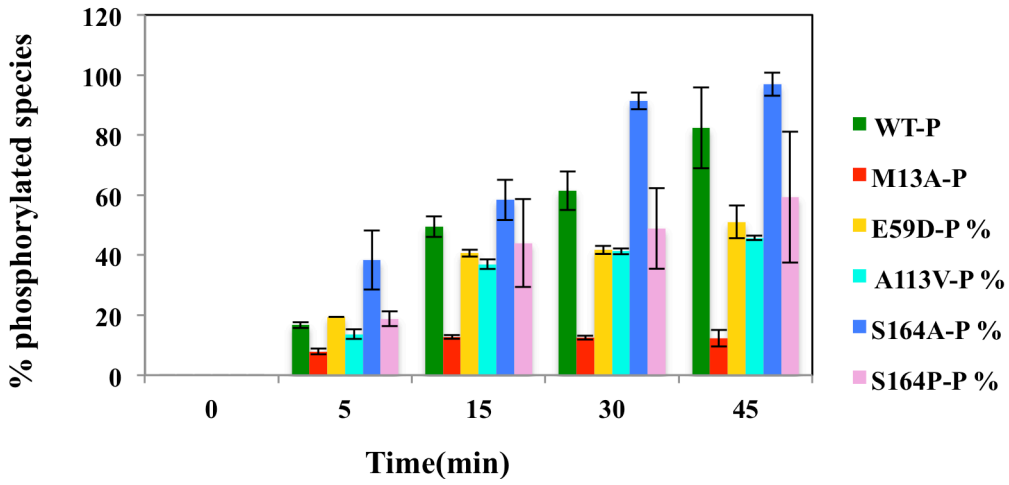

Figure 2. 6 Phos-tag gel™ quantification.
Phos-tag gel band intensities of two or three different trials were analyzed by ImageJ to determine percentage of phosphorylation in wild type as well as all the mutants. Error bars indicate standard error of mean calculated from three independent experiments.

2.3.4 Analyzing the oligomerization state

Native- PAGE was performed to investigate protein's dimerization ability after phospohrylation. Dr. Golemi-Kotra's Laboratory has reported that phosphorylation induces dimerization of VraR. Accordingly, Native-PAGE analysis showed that under the similar conditions, VraR M13A did not form dimer unlike the wild type. However all other mutants behaved same as the wild type by forming the second band as a dimer (Figure 2.7).

a. WT

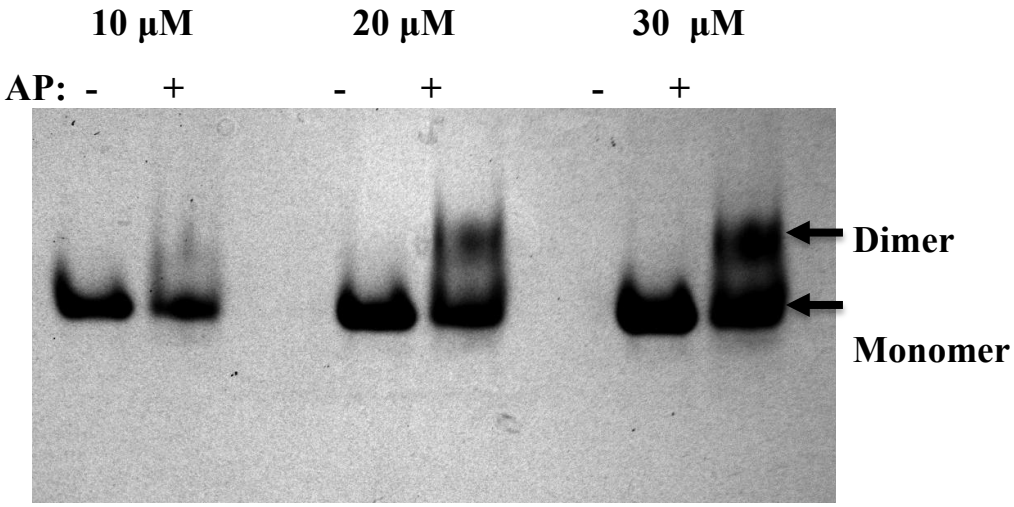

b. M13A

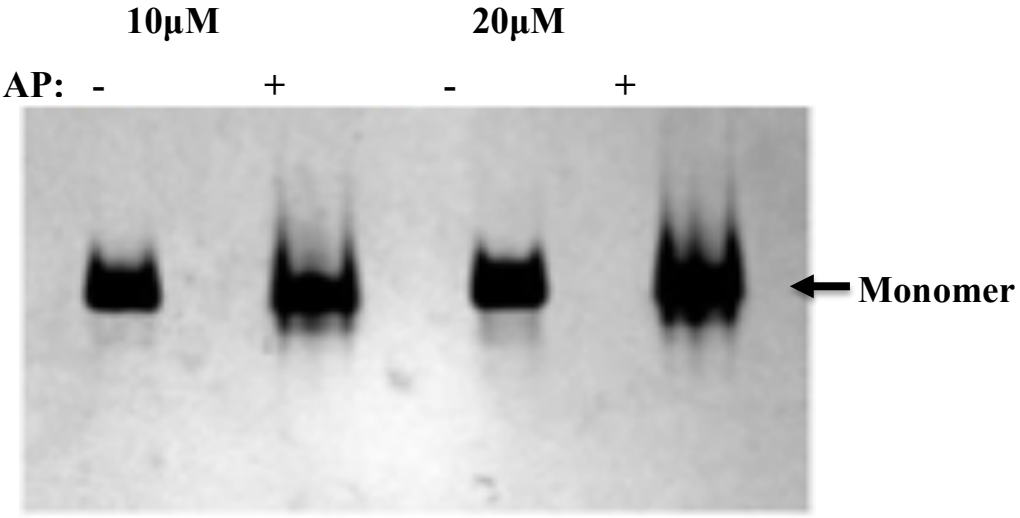

c. E59D

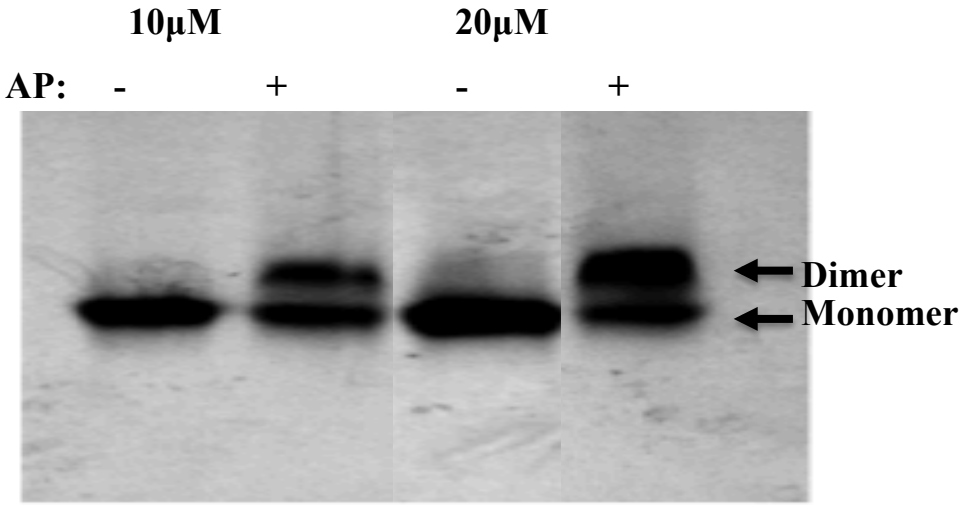

d. S164P

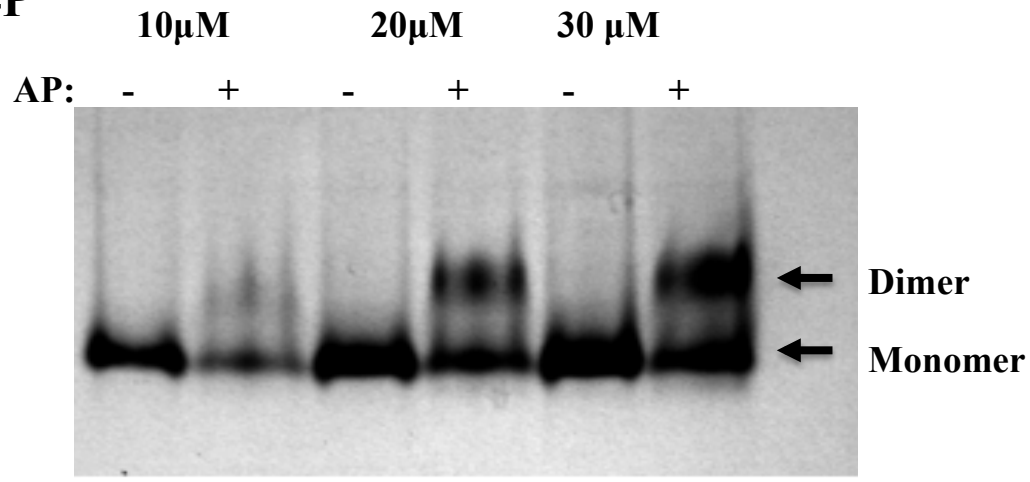

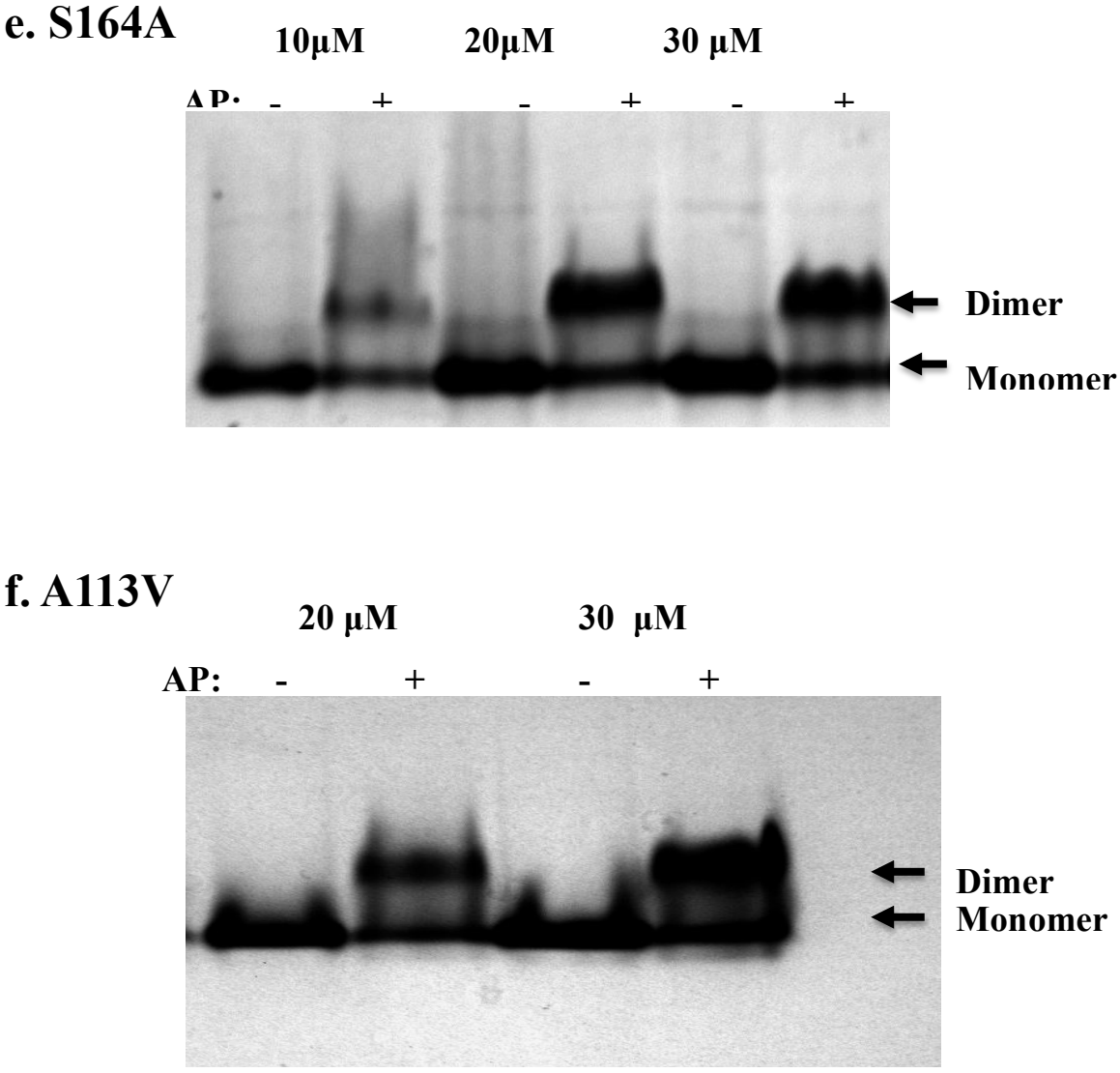

Figure 2. 7 Dimerization analysis of non-phosphorylated (NP) and phosphorylated (P) VraR wild type and mutants by 10% NATIVE PAGE

(a) VraR WT (10 µM and 20µM) and the same concentration of phospohrylated VraR WT by 50 mM acetyl phosphate were analyzed by 10% native gel. **(b)** VraR-M13A (10 µM and 20 µM) in both P and NP versions. **(c)** VraR-E59D M13A (10 µM and 20µM) in both P and NP versions. **(d)** VraR-S164P (10 µM, 20, and 30µM) in both P and NP versions. **(e)** VraR S164A (10 µM, 20, and 30µM) in both P and NP versions. **(f)** VraR S164A (10 µM, 20, and 30µM) in both P and NP versions.

2.3.5 Phosphotransfer reaction from VraS-GST to VraR

Phosphotransfer reaction from GST-VraS to VraR in the presence of [γ-^{32}P]- ATP was observed *in vitro*. About 70% of VraR wild type was phosphorylated by VraS within the first 30 second as shown by Belcheva, A., & Golemi-Kotra, D., 2008. Upon VraS phosphatase activity after 3 min the gradual decrease in VraR phosphorylation was observed that was completed after at least 10 min. Similar observations were made for the VraR variants, which were indicative of similar phosphorylation activity in both wild type and mutants, however the mutants' de-phosphorylation other than M13A occurred faster (Figure 2.8), (Next Page).

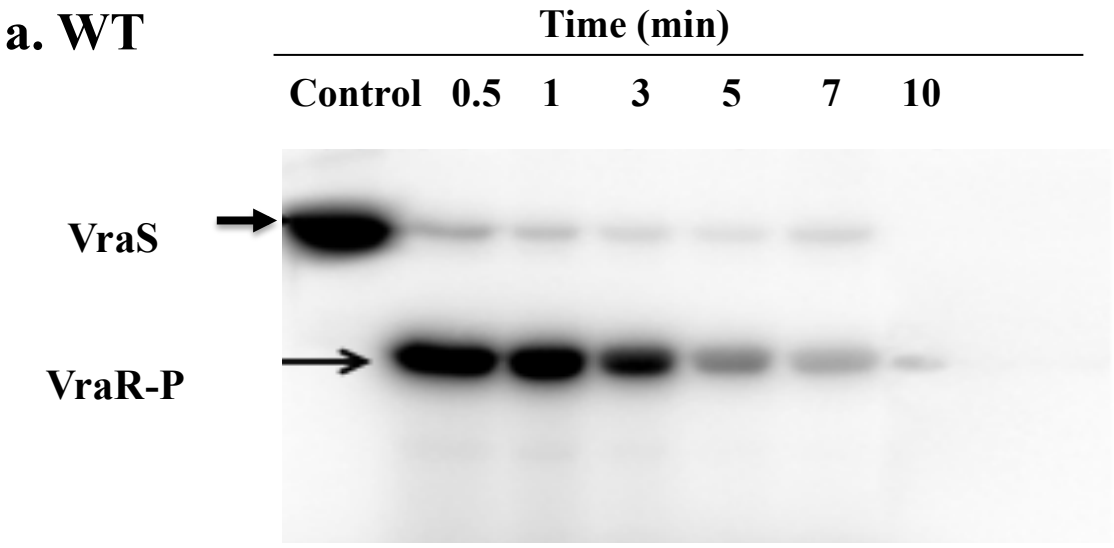
a. WT
Time (min)
Control 0.5 1 3 5 7 10
VraS
VraR-P

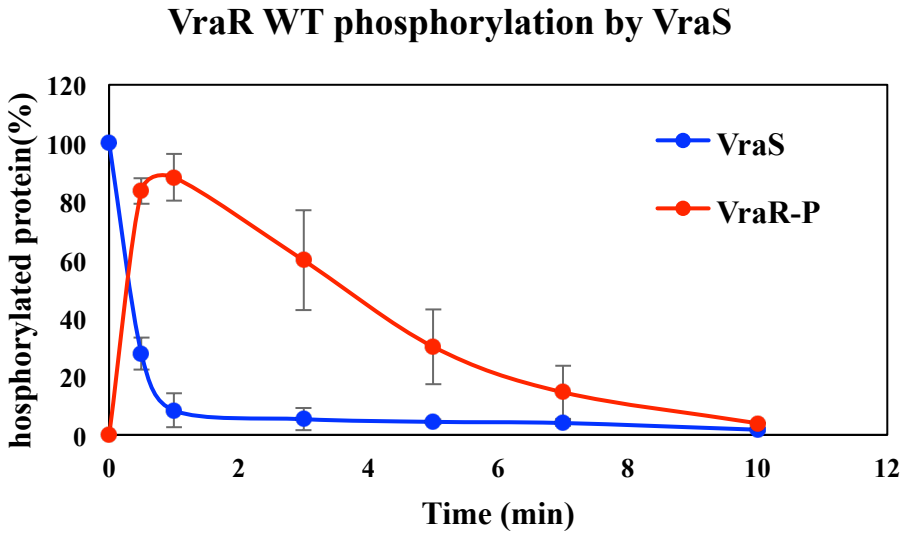
VraR WT phosphorylation by VraS
hosphorylated protein(%)
120
100
80
60
40
20
0
0
2
4
6
8
10
12
Time (min)
VraS
VraR-P

b. M13A

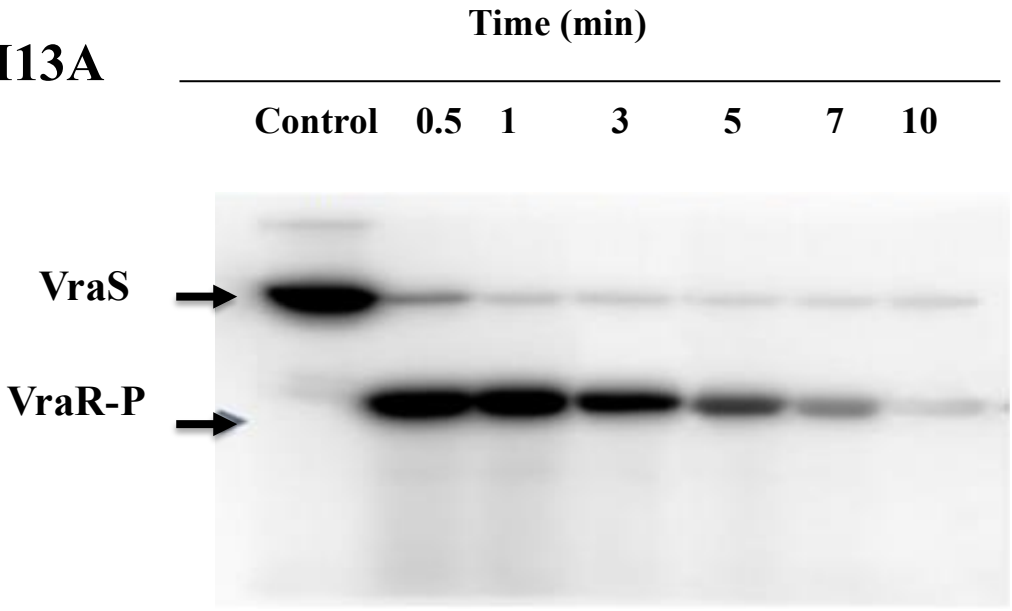
Time (min)
Control 0.5 1 3 5 7 10
VraS
VraR-P

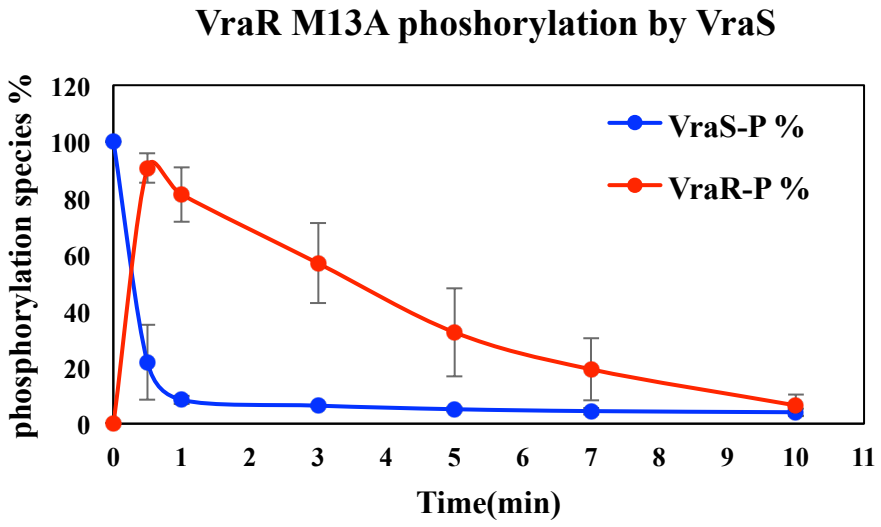
VraR M13A phoshorylation by VraS
phosphorylation species %
120
100
80
60
40
20
0
0 1 2 3 4 5 6 7 8 9 10 11
Time(min)
VraS-P %
VraR-P %

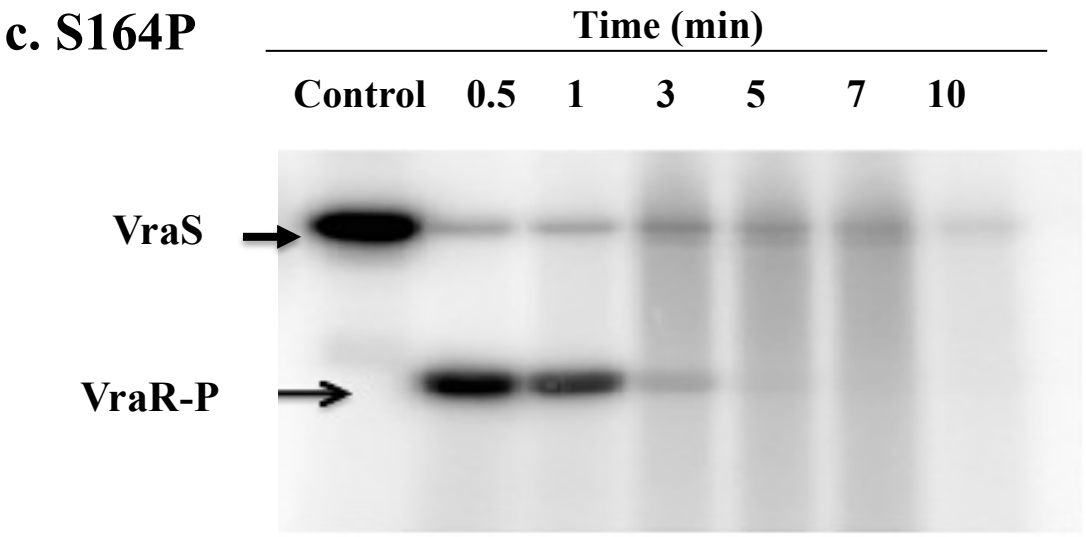
c. S164P
Time (min)
Control 0.5 1 3 5 7 10
VraS
VraR-P

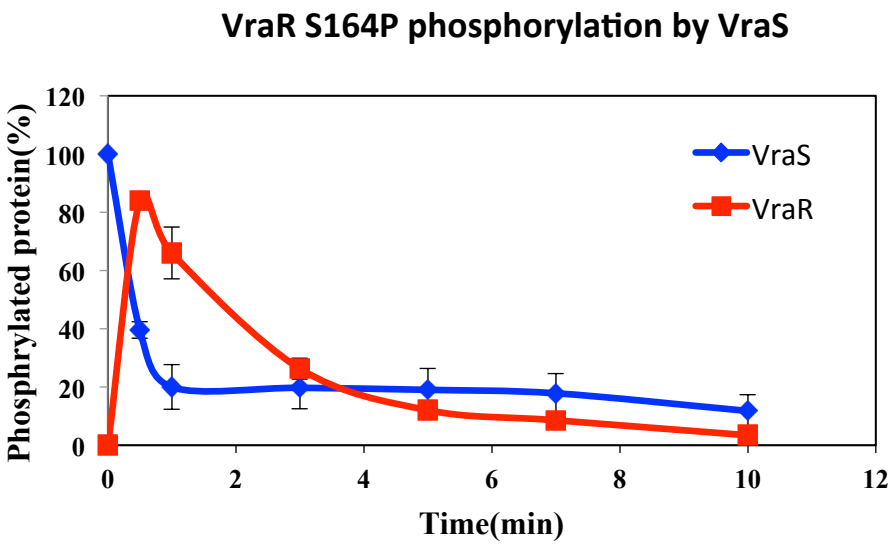
VraR S164P phosphorylation by VraS
Phosphrylated protein(%)
120
100
80
60
40
20
0
0
2
4
6
8
10
12
Time(min)
VraS
VraR

d. E59D

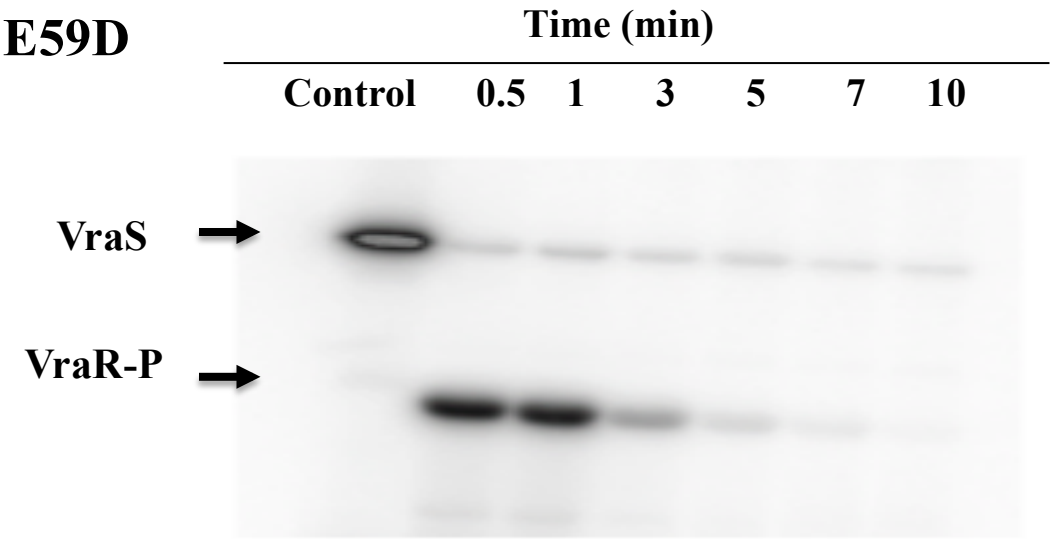
Time (min)
Control
0.5
1
3
5
7
10
VraS
VraR-P

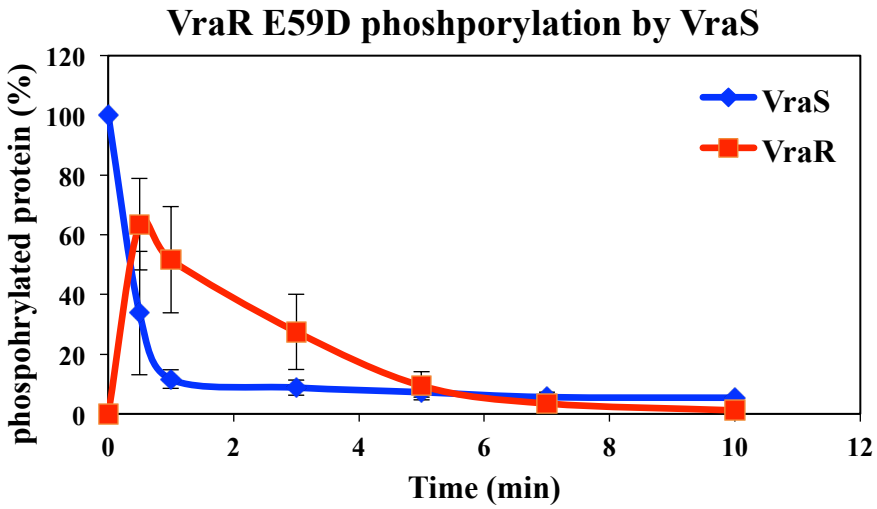
VraR E59D phoshporylation by VraS
phospohrylated protein (%)
120
100
80
60
40
20
0
0
2
4
6
8
10
12
Time (min)
VraS
VraR

e. S164A

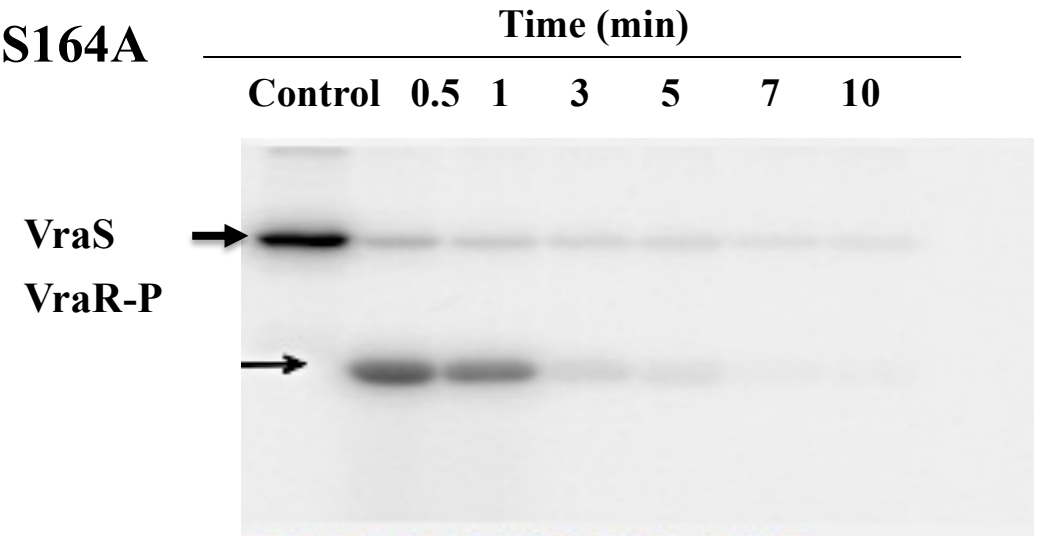
Time (min)
Control 0.5 1 3 5 7 10
VraS
VraR-P

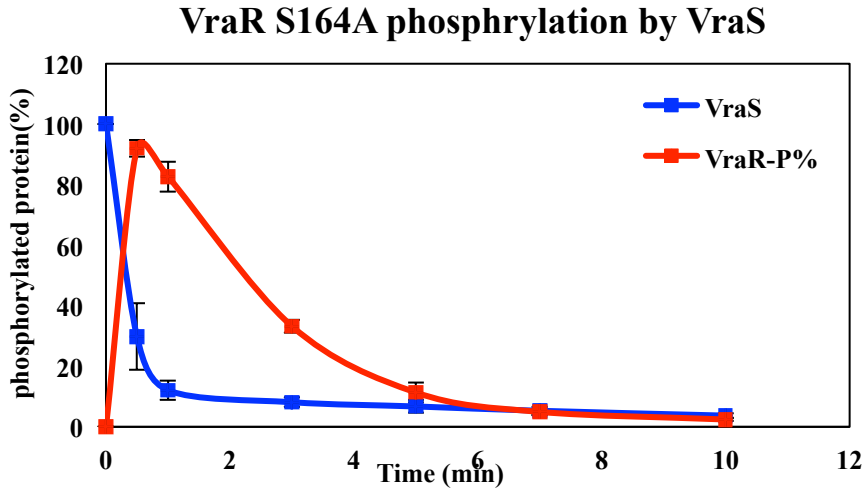
VraR S164A phosphrylation by VraS
phosphorylated protein(%)
120
100
80
60
40
20
0
0
2
4
6
8
10
12
Time (min)
VraS
VraR-P%

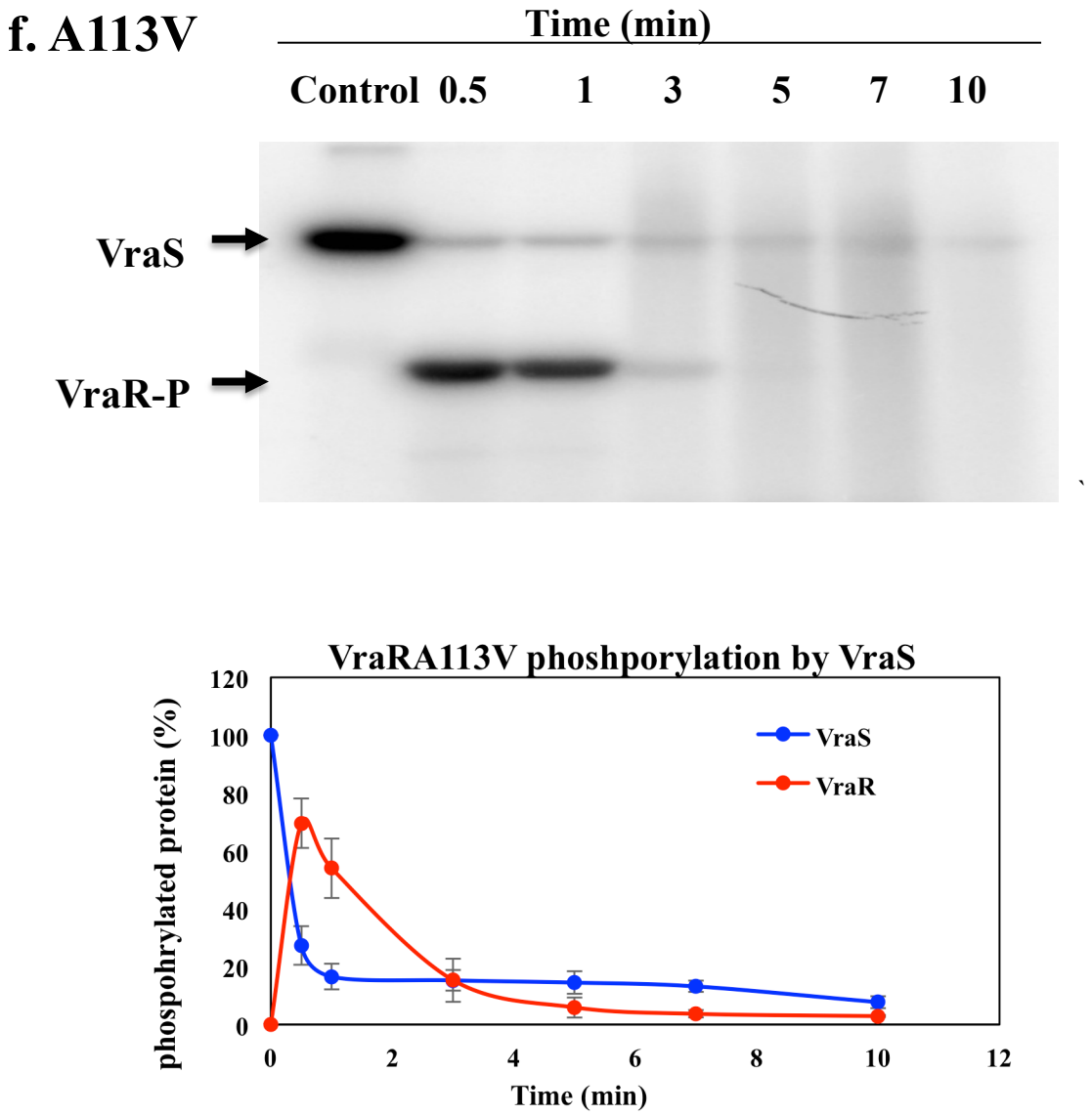

Figure 2. 8 VraR Wild type and mutants' phosphorylation by VraS-P in time intervals and their quantification graphs

20 µM VraS was incubated by radioactive ATP (3000µCi) at RT for 1h and added to 20 µM VraR and quenched by an SDS loading dye

Upper bands represent VraS autophosphorylation /dephosphorylation at the same time

Lower bands are VraR phosphorylation by VraS

VraS-P band intensities were measured using ImageJ software among three different trials and their mean percentage calculated and plotted against time versus VraR-P percentage. **(a)** VraR WT, **(b)** VraR M13A, **(c)** VraR S164P, **(d)** VraR E59D, **(e)** VraR S164A, **(f)** VraR A113V

Lane1: VraS control (No VraR was added), lane2-7: time intervals that the VraS/VraR reactions were quenched by an SDS loading dye

2.3.6 DNase-I footprinting analysis

Previous studies on VraR DNase-I footprinting revealed that unphosphorylated VraR binds to a single binding site spanned from -50 to -75 (R1 region) while the phosphorylated one can bind to an additional site between -46 to -26 (R2 region), (Belcheva A. *et al*., 2009). Repeating the experiment for the wild type demonstrated the same results. Regarding the VraR mutants, certain protected regions were observed. In case of protecting the DNA, some mutants behaved differently and some followed the VraR wild type pattern. Both unphospohrylated and phosphorylated versions of VraR M13A, which showed disability in dimerization, protected its promoter in a similar way to unphosphorylated wild type from -50 to -75 of the top DNA strand (Figure 2.9). Intensities of 3 to 4 bands in the protected region were measured for 3 different trials at different VraR concentrations utilizing ImageJ software. Subsequently, percentage of the protected DNA was plotted against protein concentration. According to the Figure 2.10, the M13A showed the least percentage of protection among all mutants. In the absence of acetyl phosphate, replacement of Glu-59 by Asp reduced non-phosphorylated VraR binding activity as well as its phosphorylated version (Figure 2.11 and Figure 2.12). A113V footprinting gel picture demonstrated that, due to VraR phosphorylation, there is an additional protected area, however, the NP-A113V protected region is approximately similar to the wild type mostly in the highest protein concentration (Figure 2.13 and Figure 2.14). The VraR C-terminal mutations (S164P and S164A) reduced the unphosphorylated protein binding activity. Both phosphorylated VraR S164P and S164A protected vraSR promoter at the additional R2 region, (Figures 2.15, 2.16 and Figures 2.17, 2.18).

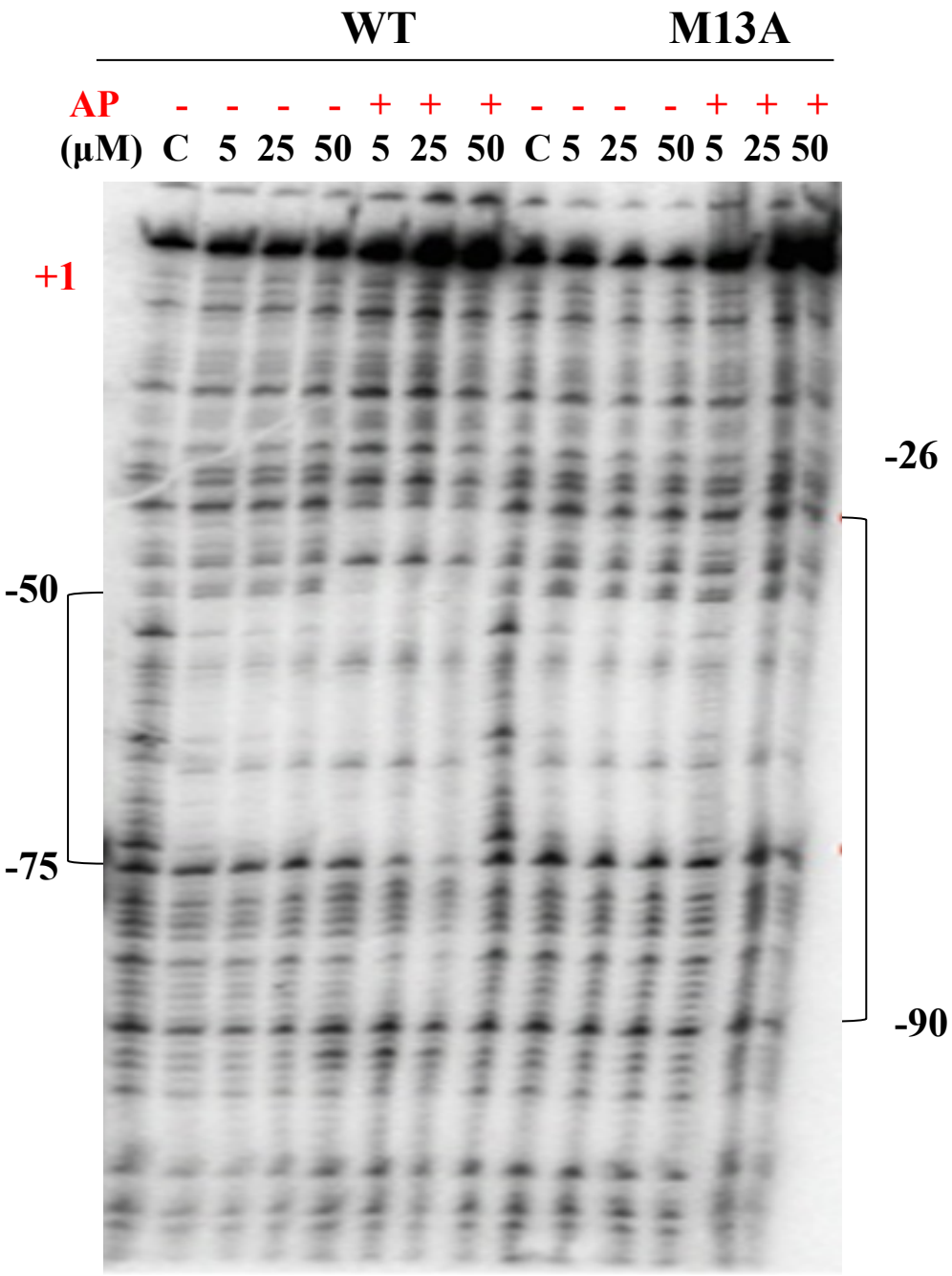

Figure 2. 9 VraR WT/M13A DNase-I fooprinting on top strand
Lanes 1,8 are the controls having no protein, Lanes 2-7 are VraR WT having different VraR concentrations: Lanes 2-4 are unphosphorylated protein (5,25,and 50 uM), Lanes 5-7 are phosphorylated protein (5,25,and 50 uM), Lanes 9-14 are VraR M13A having different VraR concentrations: Lanes 9-11 are unphosphorylated VraR (5,25,and 50), lanes 12-14 are phosphorylated VraR (5,25,and 50)

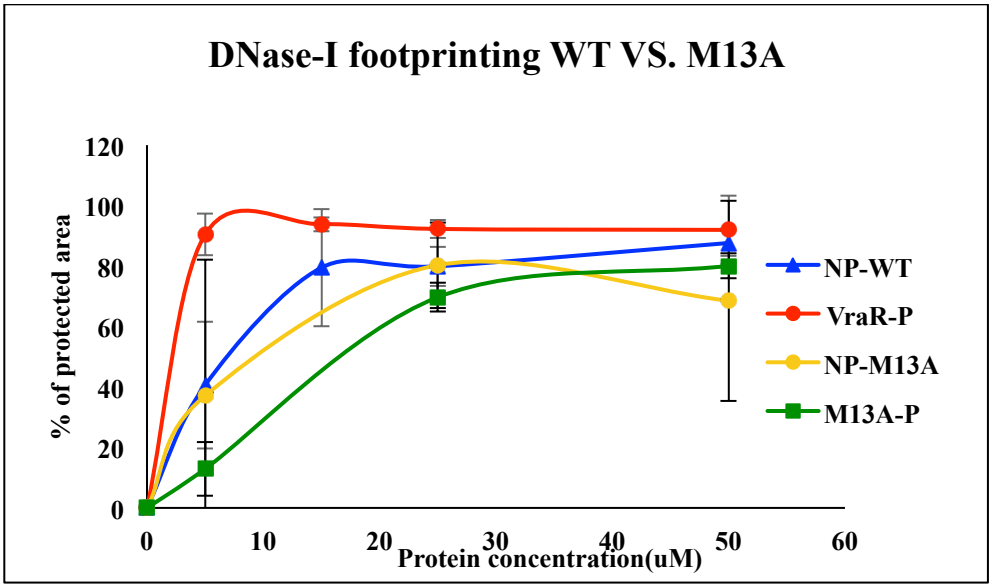

Figure 2. 10 Quantification of wild type and M13A DNase I footprinting data
Percentage of protected DNA in the region 75 to -50 is plotted against protein concentration. The intensity of three to four most prominent bands in the protected regions was measured by ImageJ software and averaged them out to calculate the protected DNA percentage. Error bars indicate standard error of mean calculated from three independent experiments.

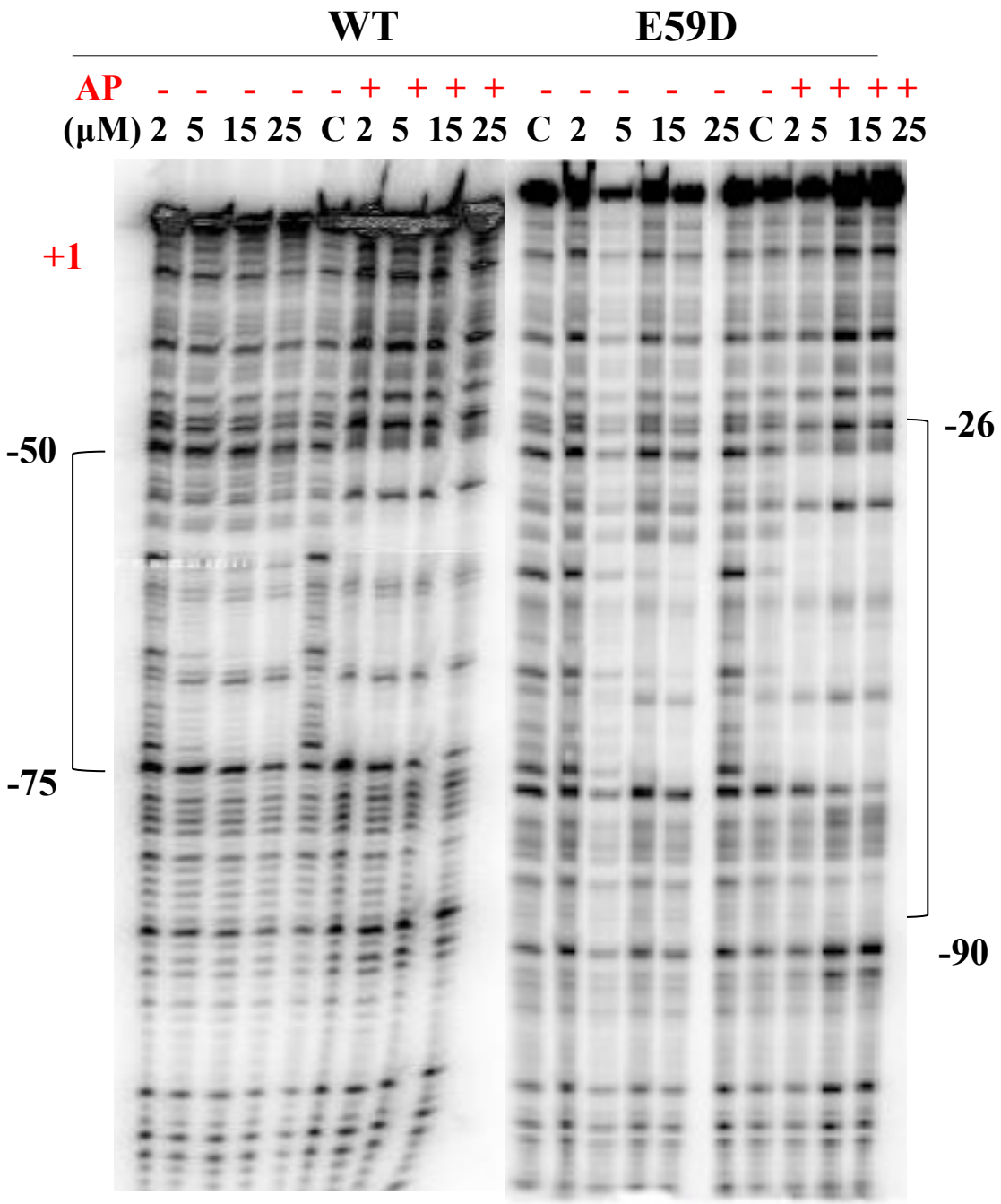

Figure 2. 11 VraR WT/E59D DNase-I fooprinting on top strand
Lanes 5,10, and 15 are the controls having no protein, Lanes 1-9 are VraR WT having different VraR concentrations: Lanes 1-4 are unphosphorylated protein (2,5,15, and 25 uM), Lanes 6-9 are phosphorylated protein (2,5,15, and 25 uM) , Lanes 11-19 are VraR E59D having different VraR concentrations: Lanes 11-14 are unphosphorylated VraR (2,5,15, and 25 uM), lanes 15-19 are phosphorylated VraR (2,5,15, and 25 uM)

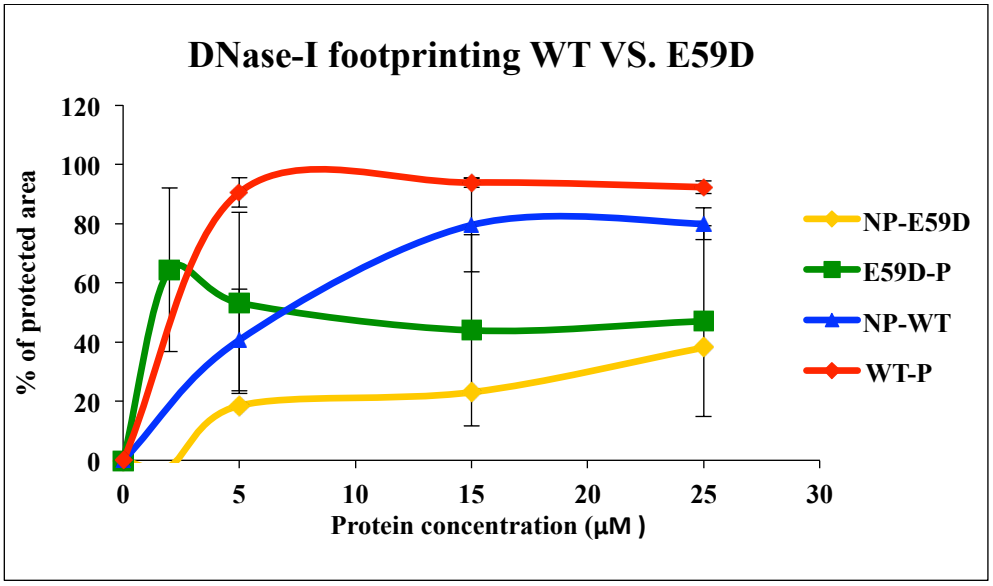

Figure 2. 12 Quantification of wild type and E59D DNase I footprinting data
Percentage of protected DNA in the region 75 to -50 is plotted against protein concentration. The intensity of three to four most prominent bands in the protected regions were measured by ImageJ software and averaged them out to calculate the protected DNA percentage. Error bars indicate standard error of mean calculated from three independent experiments.

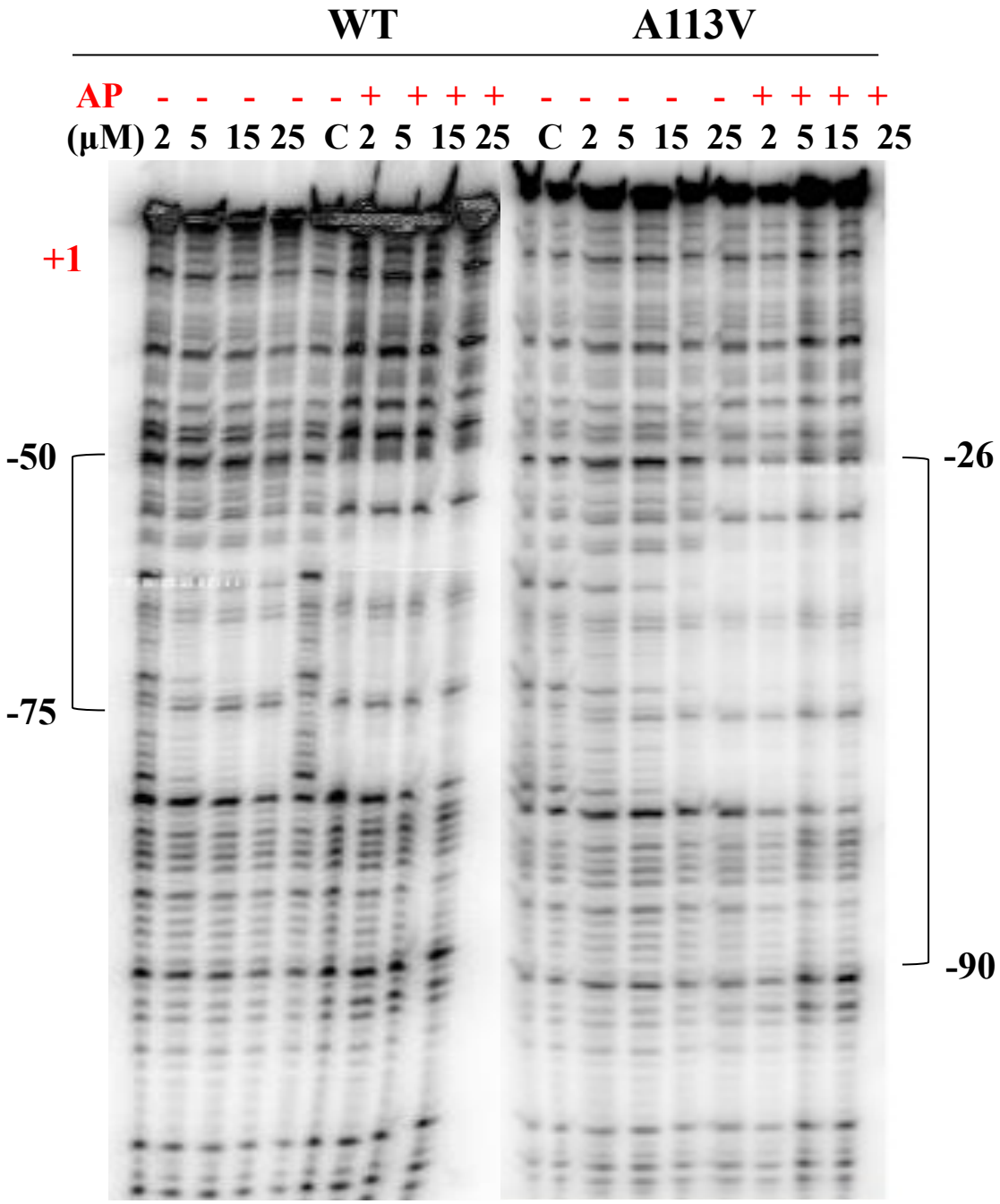

Figure 2. 13 VraR WT/A113V DNase-I fooprinting on top strand
Lanes 5,10 are the controls having no protein, Lanes 1-9 are VraR WT having different VraR concentrations: Lanes 1-4 are unphosphorylated protein (2,5,15, and 25 uM), Lanes 6-9 are phosphorylated protein (2,5,15, and 25 uM) , Lanes 11-19 are VraR A113V having different VraR concentrations: Lanes 11-14 are unphosphorylated VraR (2,5,15, and 25 uM), lanes 15-19 are phosphorylated VraR (2,5,15, and 25 uM)

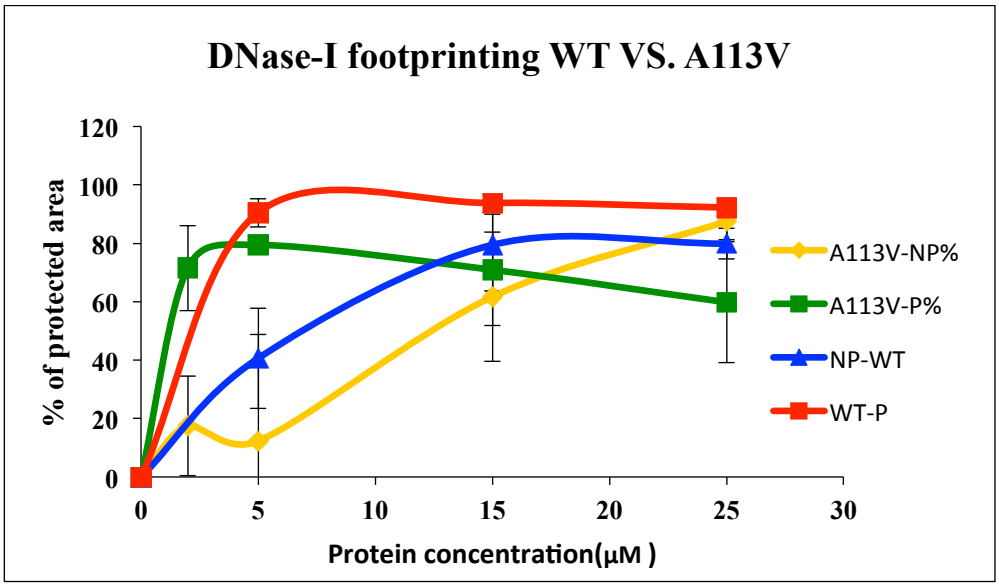

Figure 2. 14 Quantification of wild type and A113V DNase I footprinting data
Percentage of protected DNA in the region 75 to -50 is plotted against protein concentration. The intensity of three to four most prominent bands in the protected regions was measured by ImageJ software and averaged them out to calculate the protected DNA percentage. Error bars indicate standard error of mean calculated from three independent experiments.

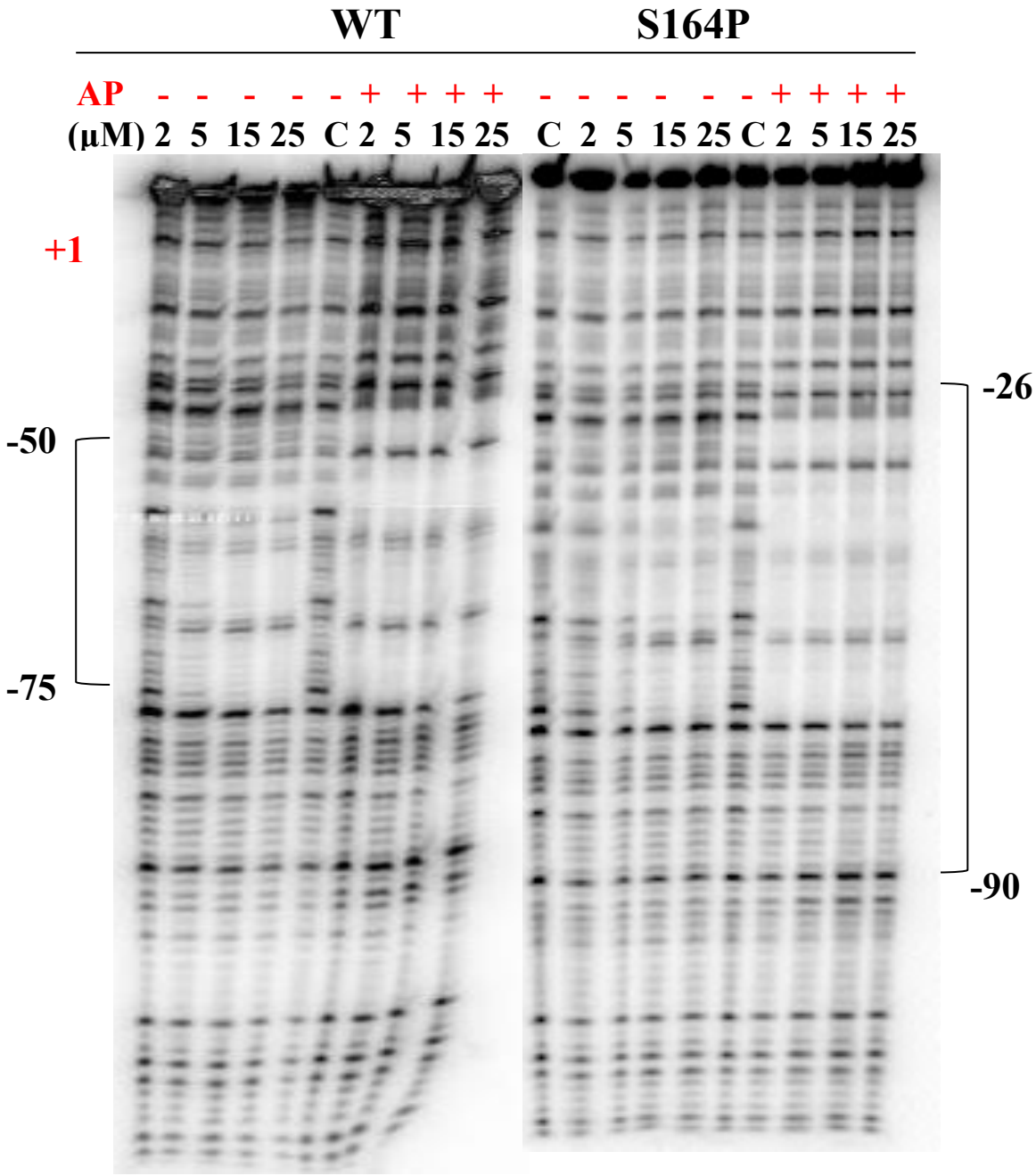

Figure 2. 15 VraR WT/S164P DNase-I fooprinting on top strand
Lanes 5,10, and 15 are the controls having no protein, Lanes 1-9 are VraR WT having different VraR concentrations: Lanes 1-4 are unphosphorylated protein (2,5,15, and 25 uM), Lanes 6-9 are phosphorylated protein (2,5,15, and 25 uM) , Lanes 11-19 are VraR S164P having different VraR concentrations: Lanes 11-14 are unphosphorylated VraR (2,5,15, and 25 uM), lanes 16-19 are phosphorylated VraR (2,5,15, and 25 uM)

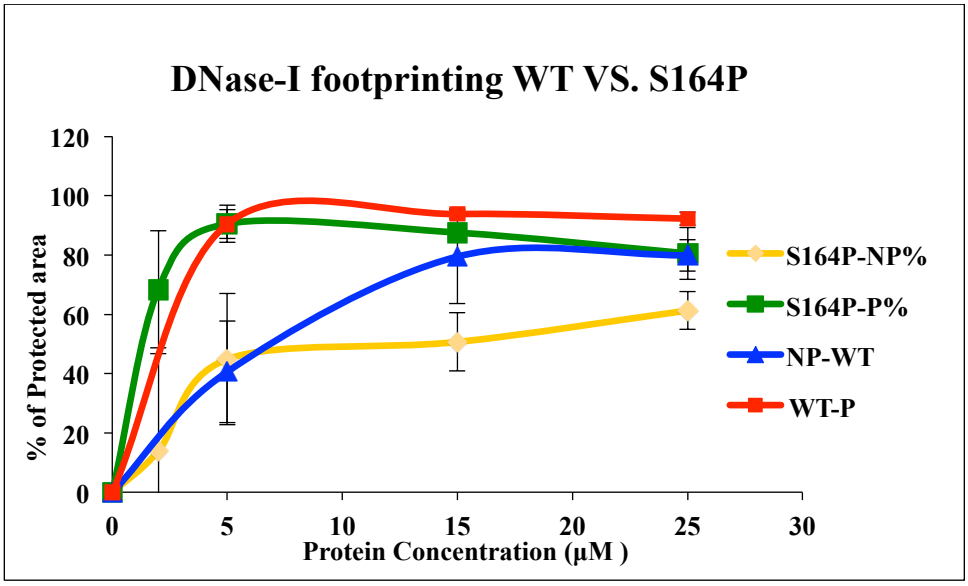

Figure 2. 16 Quantification of wild type and E59D DNase I footprinting data
Percentage of protected DNA in the region 75 to -50 is plotted against protein concentration. The intensity of three to four most prominent bands in the protected regions was measured by ImageJ software and averaged them out to calculate the protected DNA percentage. Error bars indicate standard error of mean calculated from three independent experiments.

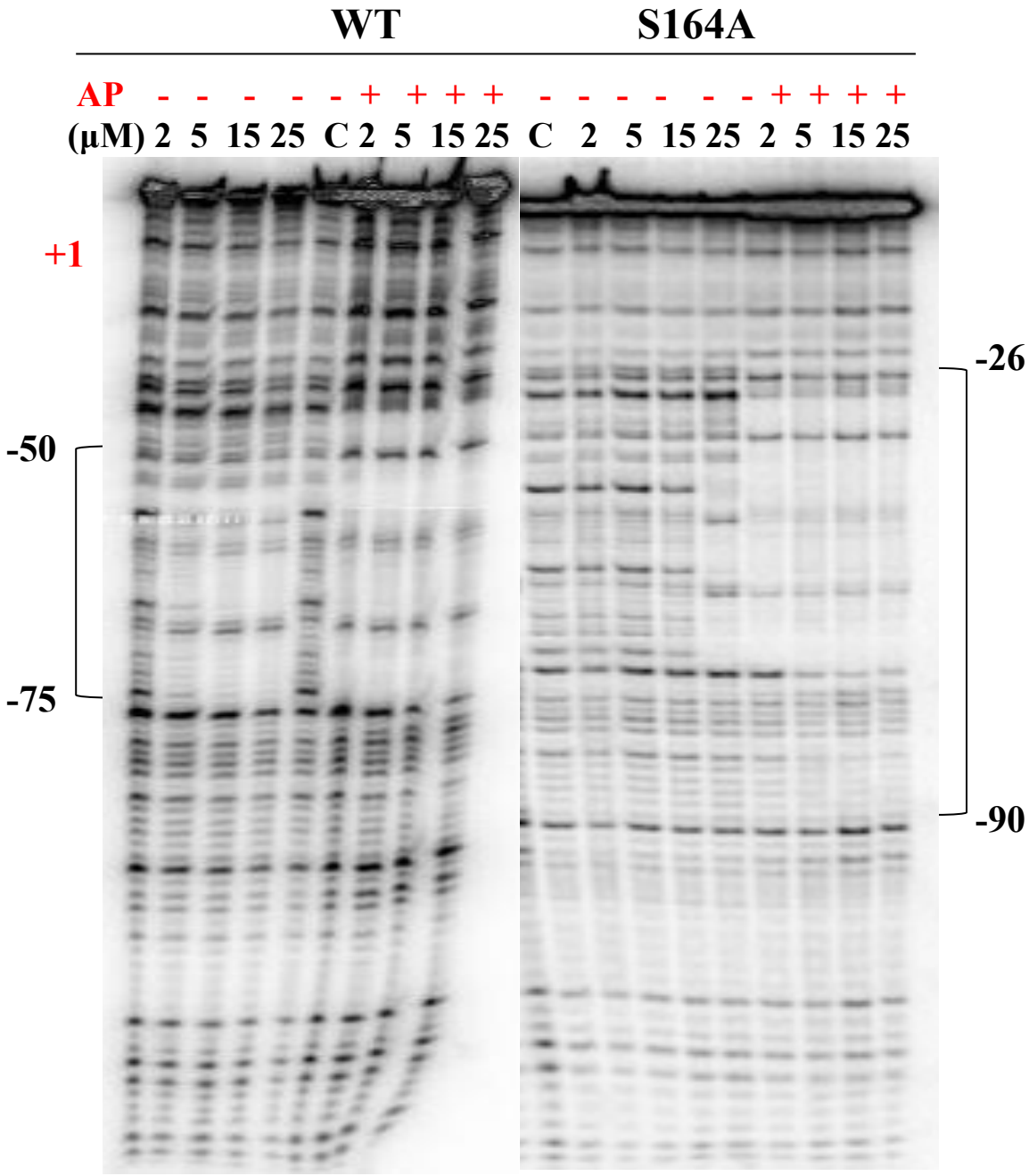

Figure 2. 17 VraR WT/S164A DNase-I fooprinting on top strand.
Lanes 5,10 are the controls having no protein, Lanes 1-9 are VraR WT having different VraR concentrations: Lanes 1-4 are unphosphorylated protein (2,5,15, and 25 uM), Lanes 6-9 are phosphorylated protein (2,5,15, and 25 uM) , Lanes 11-19 are VraR S164P having different VraR concentrations: Lanes 11-14 are unphosphorylated VraR (2,5,15, and 25 uM), lanes 16-18 are phosphorylated VraR (2,5,15, and 25 uM)

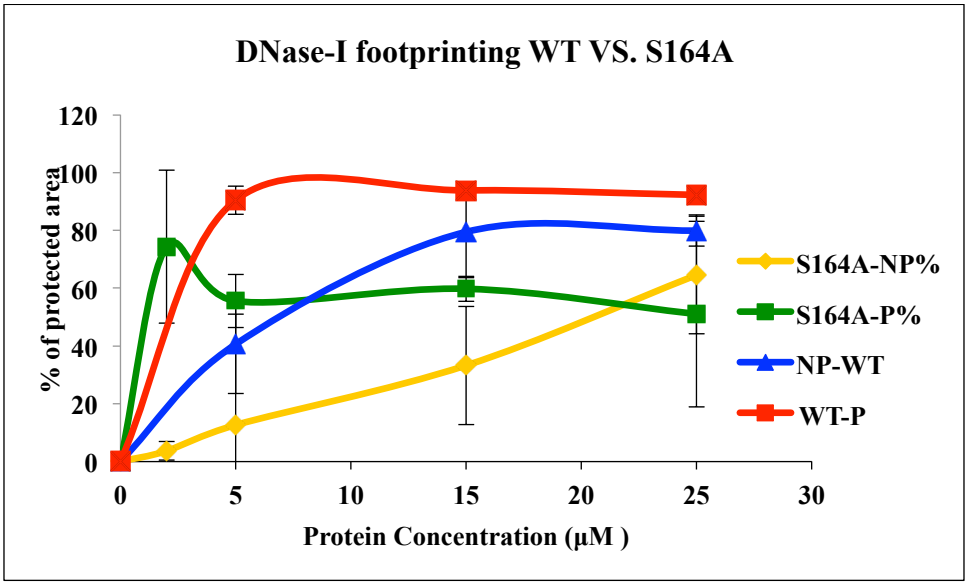

Figure 2. 18 Quantification of wild type and S164A DNase I footprinting data
Percentage of protected DNA in the region 75 to -50 is plotted against protein concentration. The intensity of three to four most prominent bands in the protected regions was measured by ImageJ software and averaged them out to calculate the protected DNA percentage. Error bars indicate standard error of mean calculated from three independent experiments.

2.3.7 Q-RT-PCR of *S.aureus* RN4220

RN4220Δ*vraR* strain was provided to our lab by Dr. Ambrose Cheung (Dartmouth College, US). Therefore, cloning of *vraSR* promoter and *vraR* gene in pMK4 and transforming into the *S.aureus* cells were done to mimic the physiological conditions (Figure 2.19). Furthermore, q-RT-PCR was done to investigate different genes expression within VraR regulon in wild type and mutant strains.

For this section we are reporting the qualitative data only due to the non-reproducible data achievement. In the current study, selected genes expression was monitored in oxacillin treated and non-treated *S. aureus* RN4220 Δ*vraR* complemented with VraR wild type or VraR mutants using q-RT-PCR. The expression was then compared to RN4220 wild type. Accordingly, the background level of *fmtA* expression was high in RN4220Δ*vraR*_(*vraR* E59D::PMK4) in the absence of oxacillin and even more higher in the presence of antibiotic. Similar expression was observed for RN4220Δ*vraR*_(*vraR* S164P::PMK4) which was higher than wild type in both treated methods. However, *fmtA* expression in RN4220Δ*vraR*_(*vraR* M13A::PMK4) was down-regulated all the time (Table 2.3).

The *pbp2* gene expression in RN4220 strain up-regulated after oxacillin treatment similar to the complementary strain. RN4220Δ*vraR*_(*vraR* S164P::PMK4) demonstrated a slightly higher expression of *pbp2* in the non-oxacillin condition while in the oxacillin treatment circumstance, slight down-regulation was observed. Same behaviour was demontrated in RN4220Δ*vraR*_(*vraR* E59D::PMK4). However, the level of *pbp2* transcription in RN4220Δ*vraR*_(*vraR* M13A::PMK4) down-regulated, and it was quite

similar to the wild type in the non-oxcillin condition (Table 2.4). This could confirm the *in vitro* experiment on the VraR-M13A protein that did not function properly.

Table 2. 3 *fmtA* expression (in comparison to RN4220 strain)

Strains/treatment types	Non-OX/WT	OX/WT
RN4220Δ*vraR*_(*vraR*::pMK4)	—	—
RN4220Δ*vraR*_(*vraR* M13A::PMK4)	↓	↓
RN4220Δ*vraR*_(*vraR* E59D::PMK4)	↑	↑
RN4220Δ*vraR*_(*vraR* S164P::PMK4)	↑	↑

Table 2. 4 *pbp2* expression level (in comparison to RN4220 strain)

Strains/treatment types	Non-OX/WT	OX/WT
RN4220ΔvraR_(vraR::pMK4)	—	—
RN4220ΔvraR_(vraR M13A::PMK4)	Same or ↓	↓
RN4220ΔvraR_(vraR E59D::PMK4)	↑	↓
RN4220ΔvraR_(vraR S164P::PMK4)	↑	↓
RN4220ΔvraR_(vraR S164A::PMK4)	Same or ↑	↓

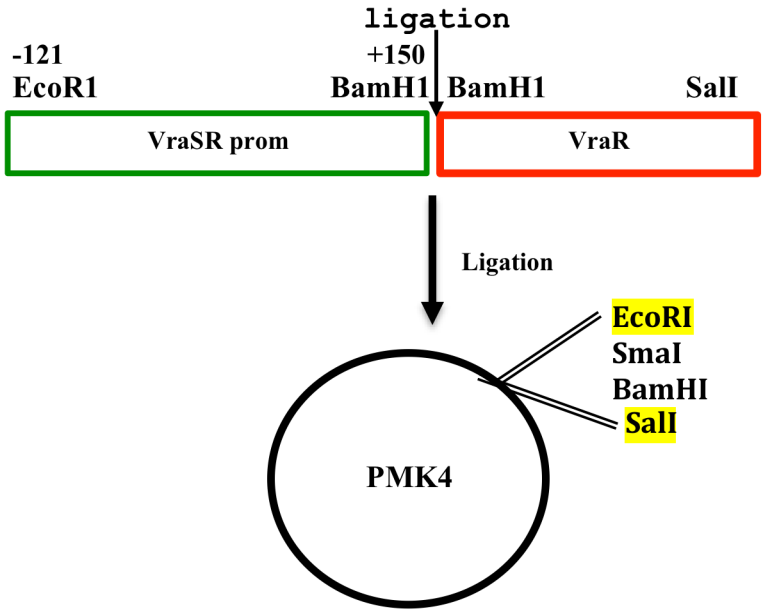

Figure 2. 19 Schematic diagram showing the pMK-4 cloning inserts and restriction sites. *vraSR* promoter from -121 to +150 with respect to the transcription start site was ligated to the *vraR* gene and as a whole segment the cloning was done in pMk-4 between EcoRi and SalI restriction sites.

2.3.8 Vancomycin MIC of RN4220 versus Δ*vraR* complemented strains

The absorbance values that have been estimated by a plate reader machine are based on the bacterial growth with an elevated OD_{600} in the particular well containing a given antibiotic concentration. The lowest MIC value is also determined by the culture that showed no bacterial growth at certain antibiotic concentration. The more intense blue color depicted by the plate reader, the higher is the OD_{600} above the baseline. Thus, the distinct antibiotic concentration is unable to inhibit bacterial growth (data are shown in Appendix B,

Figure B1).

RN4220 has an MIC between 0.5 μg/ml to 1 μg/ml towards vancomycin, whereas ΔvraR has an MIC of 0.25 μg/ml to 0.5 μg/ml (Table 2.5). The complement strains including the mutants were able to revert the MIC back to 0.5 μg/ml unlike RN4220ΔvraR_(vraR S164P::PMK4) which showed MIC between 0.25 μg/ml to 0.5 μg/ml (Table 2.5). Colony counts method on the wild type, mutant, and complementary wild type confirmed the above results (data have not shown).

Table 2. 5 Vancomycin MICs of RN4220, RN4220Δ*vraR* and complement strains. Data were collected from three different trials

Strain	Vancomycin MIC (μg/ml)
RN4220	**0.5-1**
RN4220Δ*vraR*	**0.25-0.5**
RN4220Δ*vraR*_(*vraR*::PMK4)	**0.5**
RN4220Δ*vraR*_(*vraR* M13A::PMK4)	**0.5**
RN4220Δ*vraR*_(*vraR* E59D::PMK4)	**0.5**
RN4220Δ*vraR*_(*vraR* S164P::PMK4)	**0.25-0.5**
RN4220Δ*vraR*_(*vraR* S164A::PMK4)	**0.5**

2.4 Discussion

Response regulator proteins have been proposed to be often involved in virulence pathway regulation, and help bacteria to escape from the host immune system. These proteins have also been reported as an interesting drug targets because they have no human homologs (Leonard P.G., *et al*., 2013). VraR, the transcription factor protein represents an attractive therapeutic target, as the VraSR TCS is vital for *S. aureus* resistance to any available antibiotics. Hence, studying VraR protein's structure and its DNA binding interactions could potentially restore *S. aureus* sensitivity to many antibacterial agents where resistance has become a critical worldwide concern. Here, the goal of our study was to characterize the key roles of amino acid substitutions in VraR and to examine their possible effects on VraR signal transduction. Some of the VraR mutants that were tested in this study were confirmed to be clinical strains (VraR E59D, A113V, and S164P) and were reported to contribute to glycopeptide (Vancomycin) resistance (Yoo J.I., *et al*., 2013)

VraR and its variants were successfully purified using previously described methods (Belcheva A, & Golemi-Kotra D, 2008). Then, they were further investigated to compare their biochemical nature and DNA binding abilities with wild type VraR.

To obtain further insights about the protein structural feature, circular dichroism spectra was analyzed. This technique is mainly based on the fact that optically active biomolecules, including proteins, reveal different absorptions of left and right circularly polarized light within the range of 200-260nm (Mcphie P, 2001). Therefore, secondary structures like α-helices and β-sheets would affect the CD spectrum, producing different

spectra. Further, CD technique can be used to analyze protein-folding patterns helping us define whether a protein is correctly folded, miss-folded or denatured. In our study, it was shown that the wild type and the mutant proteins have similar CD spectra. Moreover, thermal melting was performed to provide more information about potential stability of the mutant (Nakanishi, K., *et al*., 2000). The thermal melting indicated no structural alterations among the wild type and the mutants.

We used Lithium potassium acetyl phosphate *in vitro* as a phosphodonor molecule (Belcheva A, & Golemi-Kotra D., 2008), to phosphorylate VraR wild type and mutant proteins, to examine their phosphorylation and dimerization ability by Phos-tag^{TM} gel and native-gel. It is known for almost all RRs REC domains to function as a phosphorylation-activated switch. REC domains exist in equilibrium between two inactive and active states. NMR studies indicate to a microsecond equilibrium shift fluctuation between an inactive unphosphorylated REC domain and stabilize phosphorylated REC domain (Gao R, & Stock A.M, 2009). The Regulatory domain conformational changes are the result of the phosphorylation, which turns the RR from an inactive OFF to an active ON state. (Birck C, *et al*., 2002). Accordingly, the M13A mutant phosphorylation rate after 45 min was 6 folds smaller than the wild type and it failed to form dimer. This can be explained by this fact that there is a possibility that the VraR M13A switching pattern between ON and OFF is somehow inhibited. In other words, in the absence of this critical residue (Leonard P.G., *et al*., 2013), the active state would not be there, which may interfere with the acetyl phosphate dependent phosphorylation of the mutant. As an example, PhoP is a receiver domain that

gets stabilized and dimerized through phosphorylation (Menon S., & Wang S., 2011). Another study, which is performed by Rhee J.E., *et al*., 2008 on OmpR RR mutants indicated that the amino acid alteration inhibits phosphorylation in the N-terminal receiver domain. As a result, the M13A dimerization inability led to its failure of binding to its promoter, which will be discussed later. However, dimerization ability of the rest of the mutants did not get affected.

VraR S164A phosphorylation rate was significantly higher compared to the wild type after 30 min and reached to its saturated level after 45min. This could be due to the experimental errors, or it could be due to the fact that alanine is a small amino acid and its side chain is very non-reactive and is thus hardly involved in protein functions such as phosphorylation (Betts M.J, *et. al*., 2003). Nonetheless, this mutant's phosphorylation ability needs to be repeated.

Based on the VraS structure and mathematical modeling, previous studies have entitled VraS as a bifunctional kinase. Bifunctional histidine kinase is able to catalyze both the phosphorylation and dephosphorylation of its cognate response regulator (Alves R., and Savageau M.A, 2003). Many HKs have the intrinsic ability to phosphorylate their cognate RR. In this regard Belcheva A., *et al*., (2008) for the first time showed that the phosphotransfer from GST-VraS to VraR is very efficient with about 70% of the transfer taking place within the first 30 seconds. This rapid phosphotransfer was observed in all the mutants along with the wild type as a control and suggested that in the presence of cell wall stress, this system could be readily activated resulting in high levels of phosphorylated VraR

species in cell. Consequently, the amino acid substitutions in VraR did not effect the VraS-VraR interactions. In turn, phosphotransfer from VraS to VraR was not altered within 10 min.

Many RRs have an inherent skill to go through dephosphorylation, however this activity is gradual and is normally enhanced by the cognate HK or an auxillary protein. (Bilwes A.M, *et al*., 2000, Belcheva and Golemi-Kotra, 2008). This phenomenon is referred to the phosphatase activity of HK (Laub M.T., and Goulian M., 2007). Addition of VraS to the VraR-P drastically enhanced the hydrolysis of the phosphor-aspartate in VraR-P, which led to its rapid and complete dephosphorylation. Moreover, VraR-P by acetyl phosphate remained stable for about 10 hours. Several other HKs, including Enzv, FixJ, and NarX were presented to dephosphorylate their cognate RRs (Hedda U., *et al*., 2014; Diensthuber R., *et al*., 2013; Bhate M., *et al*., 2015). Accordingly, slightly faster dephosphorylation was observed for all the mutants except for the VraR M13A that behaved exactly similar to the wild type.

The results further showed that phosphorylation-induced dimerization of VraR and its variants enhanced the VraR DNA-binding affinity. DNase-I footprinting experiment was used to demonstrate the binding regions of VraR on the *vraSR* promoter or in other words predicting the ability of the protein in protecting its promoter regions against DNase-I attack. Previously, it was shown that phosphorylation has an effect on VraR conformation and DNA-binding activity. Accordingly most of the RRs dimerization upon phosphorylation leads to bring the DNA-binding domain to close proximity and bind to DNA sequences

(Menon S., and Wang S (2011). Thus, any factor that diminishes the phosphorylation-induced activation, would definitely affect its DNA binding interactions. Referring to the example earlier about the OmpR mutant's disability in dimerization, which negatively affected its DNA binding activity (Rhee J.E., *et al*., 2008). In current study, the M13A-P did not bind to the R2 phosphorylated-dependent region of its promoter. However, binding ability of E59D-P and A113V-P to the R2 region was slightly decreased as compared to the wild type. The VraR C-terminal mutations (S164A and S164P) caused a partial loss of their DNA binding ability in their unphosphorylated state, especially in low protein concentrations unlike their phosphorylated versions.

It was explained that when vancomycin MIC of *S. aueus* is lowered than ≤ 2 μg/mL counts as susceptible (CSLI, 212). Moreover, the most prevalent amino acid substitutions such as the E59D and A113V were shown to being susceptible to vancomycin, with an MIC range from 3-4 μg/mL (Yoo J., *et al*., 2013). In another study, VISA strains composed of clinical, and in-vitro strains were defined to have an MIC between 4-8 μg/ml (Alam M.T., *et al.,* 2014). The *S. aureus* RN4220 strain, used in this research is a susceptible strain and introducing only *vraR* or a single mutation in *vraR* did not convert it to a resistant strain. It shows that there might be some other factors involving in vancomycin resistance as well (Hafer C, *et al.,* 2012). Overall, it was observed that in the absence of *vraR*, the MIC goes down and introducing the *vraR* takes the MIC back to the control level. That is further enhanced by the introduction of the M13A, E59D, S164A and S164P mutations. Current MIC result showed increased-sensitivity towards vancomycin, however, Δ*vraR* complement

strains were able to revert the MIC back to the wild type level (0.5-1 μg/mL). As the MIC range is very little, but it is understood that vraSR system play a significant role in antibiotic resistance in *S.aureus* that it is better to demonstrate by an alternative method.

The q-RT-PCR analysis of *S. aureus* N315 cell wall-associated genes such as *pbp2*, *fmtA*, and *sgtB,* were shown to be upregulated in response to oxacillin, (Sengupta, M., *et al*., 2012). In current study, the *fmtA* transcription levels in the clinical strains, RN4220Δ*vraR*_(*vraR* S164P::PMK4) and RN4220Δ*vraR*_(*vraR* E59D::PMK4) observed higher compare to the wild type in both treated and non-treated conditions, unlike RN4220Δ*vraR*_(*vraR* M13A::PMK4). RN4220 and its complementary strain up-regulate the *pbpb2* transcription level as expected. The lower levels of *pbp2* in E59D, S164P and S164A compared to the wild type in the presence of oxacillin could have an impact on carbohydrate chains cross-linking process in cell-wall biosynthesis (Boyle-Varvara. S. *et al*., 2012). It is definitely necessary to repeat the q-RT-PCR experiment to obtain conclusive data. Then, if any of the genes expression increase, the will enhance peptidoglycan biosynthesis and antibiotic resistance. On the other hand, the decreased level of transcription interrupts in the cell-wall biosynthesis process leading to the antibiotic positive effect.

3 CHAPTER THREE: CONCLUSIONS AND FUTURE PERSPECTIVE

3.1 Conclusion

The discovery of TCSs happened 30 years ago and scientists have made great strides toward understanding the signal transduction mechanism. Here, we discuss specifically on the VraSR system in *S. aureus*. It has been demonstrated that how the VraSR TCS coordinates bacterial responses to the cell wall damage by modulating a set of genes and a phosphorelay mechanism (Stock AM, 2009). Transcription levels of certain genes have been shown to enhance, in the presence of peptidoglycan inhibitors at comparatively low concentrations of antibacterial agents such as vancomycin (Gardete S, *et al*., 2006; Kuroda M, *et al*., 2003).

VraR wild type was expressed and purified previously by Antoaneta Belcheva (2008) in Dr. Golemi-Kotra Laboratory. Therefore, we were able to express and purify the already generated mutants of *vraR* encoding for substitutions M13A, A113V, S164P, and S164A. The E59D substitution was also confirmed and the pure protein was isolated with the same purification method. Subsequently, to get an understanding of the role of each substitution in VraR; biochemical properties, folding pattern, potential stability of each protein was analyzed. These studies did not reveal a significant diffrence amoung the secondary structural features of VraR and its variants.

To illustrate oligomerization state and phosphorylation ability of the proteins *in vitro* the native gel analysis and the phos-tag gel™ were carried out. The phos-tag™ gel

experiment displayed the least phosphorylation rate for M13A compared to the wild type due to the inactive/active equilibrium shift (Birck C, *et al.,* 2002). Other *vraR* variants showed phosphorylation contents between 70%-80% after 45 min similar to the wild type. However, after 30 min, higher phosphorylation content was observed for VraR-S164A. So, it will be necessary that this experiment repeat for further conclusive explanation. Belcheva *et al*., (2008) indicated the VraR wild type dimerization ability upon phosphorylation previously. The native-page gel analysis determined similar behavior between wild type and mutants in dimerization ability except for VraR-M13A. The effect of Met-13 point mutation to Ala on VraR dimerization ability without any significant alterations on its biochemical properties, made us realize that it is essential to examine the DNA binding ability.

The VraS and VraR relationship in exchanging phosphoryl group was done by the radioactive [γ-^{32}P]-ATP. Earlier, our lab indicated that the wild type VraR-dependent phospohtrasfer is fast and about 70% of it occurs within 30 seconds (Belcheva A., & Golemi-Kotra D, 2008). Current research illustrated that the amino acid replacements did not alter VraR phosphorylation by VraS.

Identification of the VraR binding sites on its promoter was performed by DNase-I footprinting to point out the VraR binding activity (Belcheva A, *et.al*., 2012). The M13A substitution caused a complete loss of the VraR-P binding affinity at R2, which was in agreement with its dimerization disability. The loss of binding definitely has an impact on the expression of the related genes regulation in the stress condition. In all mutants the non-phosphorylated proteins protected their DNA in much lesser extent than the wild type,

which of VraR S164A, S164P, and E59D are the least ones. The rest of the phosphorylated mutants protected the R2 region but in a slight lower level than the wild type. Nonetheless, in this study, the VraR amino acid manipulations, slightly reduced or disabled proteins' binding affinity to their DNA.

According to the *in vivo* studies, *vraSR* promoter and *vraR* gene were cloned into pMK-4 properly, and RN4220 transformation mimicked physiological conditions to examine q-RT-PCR analysis and vancomycin minimum inhibitory concentrations.

q-RT-PCR was used for certain cell-wall-associate genes known to be upregulated under oxacillin treatment (Sengupta, M, *et al*., 2012). We demonstrated qualitative outcomes due to the non-reproducible data, and compared each strain within its category along with the wild type control: antibiotic treatments versus RN4220-wild type and non-antibiotic treatments versus RN4220-wild type. This experiment needs further analysis in order to achieve conclusive and quantitative data.

MICs of the susceptible strains showed the ability of complementary strains to bring the MIC back to the wild type (RN4220) unlike the RN4220Δ*vraR*. Because of the small range of MIC concentration, it is still necessary to confirm the effect of mutations in an alternative way.

3.2 Future perspective

The observation that the VraR-M13A does not form any dimers upon phosphorylation and loses its binding ability to the R2 region is certainly an interesting one. We have provided solid evidence that this mutation inhibits the expected VraR role as a transcription factor. Also, it is remarkable that the mRNA level of this mutant's cell-wall-associated genes was downregulated in both oxacillin and non-oxacillin conditions. Thereupon, it is also worth to examine the cell-wall-associated genes expression under vancomycin introduction not only in this complementary strain but also in all the mutated complement strains. Consequently, we will be able to be more conclusive about the current *in vivo* studies. Future work can also focus on the effect of these amino acid alterations on the cell growth pattern by subjecting the antibiotics.

It is also interesting to find any other key residues in the VraR protein, and by doing multiple mutations at a time, analyze any possible outcomes, from their structural stability to the promoter protection ability. VraR-A113V mutant, a clinical *S. aueus* strain, still needs to be studied *in vivo* using q-RT-PCR and MIC.

I am also interested in to observe the consequences of the VraT and VraR mutation simultaneously. It has been shown that VraT has an inhibitory element on LiaR protein in *B. subtilis*, the VraR homolog (Boyle-Varvara. S. *et al*., 2012). So, what would be the effects of the VraT /VraR amino acid changes on the VraSR system.

At last, it is necessary to put more efforts and researches towards understanding the VraSR two-component system. Therefore, it may make us closer to our ultimate goal,

producing effective antibacterial agents against *S. aureus* resistance strains.

4 REFERENCES

Alam, M. T., Petit, R. A., Crispell, E. K., Thornton, T. A., Conneely, K. N., Jiang, Y., Read, T. D. (2014). Dissecting Vancomycin-Intermediate Resistance in Staphylococcus aureus Using Genome-Wide Association. *Genome Biology and Evolution, 6*(5), 1174-1185.

Alves, R. and M. A. Savageau (2003). Comparative analysis of prototype two-component systems with either bifunctional or monofunctional sensors: differences in molecular structure and physiological function. *Mol Microbiol* 48(1): 25-51

Belcheva, A., Golemi-kotra, D. (2008) A Close-up View of the VraSR Two-component System: A mediator of staphylococcus aureus response to cell wall damage. *Journal of biological chemistry*. *283*,12354-12364

Belcheva, A., Verma, V., Golemi-Kotraa, D., **(**2009) DNA-Binding Activity of the Vancomycin Resistance Associated Regulator Protein VraR and the Role of Phosphorylation in Transcriptional Regulation of the vraSR Operon, *Biochemistry,* 48, 5592–5601

Belcheva, A., Verma, V., Korenevsky, A., Fridman, M., Kumar, K., & Golemi-Kotra, D. (2011). Roles of DNA Sequence and Sigma A Factor in Transcription of the vraSR Operon. *Journal of Bacteriology,194*(1), 61-71.

Bell, J. M., & Turnidge, J. D. (2002). High Prevalence of Oxacillin-Resistant Staphylococcus aureus Isolates from Hospitalized Patients in Asia-Pacific and South Africa: Results from SENTRY Antimicrobial Surveillance Program, 1998-1999. *Antimicrobial Agents and Chemotherapy, 46*(3), 879-881.

Betts, M. J., & Russell, R. B. (n.d.). Amino-Acid Properties and Consequences of Substitutions. *Bioinformatics for Geneticists,* 311-342.

Bhate, M., Molnar, K., Goulian, M., & Degrado, W. (2015). Signal Transduction in Histidine Kinases: Insights from New Structures. *Structure, 23*(6), 981-994

Bilwes, A. M., L. A. Alex, B. R. Crane and M. I. Simon (1999). Structure of CheA, a signal-transducing histidine kinase. *Cell* **96**(1): 131-141.

Birck,C., Malfois, M., Svergun, D., and Samama, J. (2002) Insights into signal transduction revealed by the low resolution structure of FixJ response regulator. *J Mol Biol 321,* 447-457

Bobay, B. G., Hoch, J. A., & Cavanagh, J. (2012). Dynamics and activation in response regulators: the β4-α4 loop. *Biomolecular Concepts, 3*(2)

Boyle-Vavra, S., Yin, S., Jo, D. S., Montgomery, C. P., & Daum, R. S. (2012). VraT/YvqF Is Required for Methicillin Resistance and Activation of the VraSR Regulon in Staphylococcus aureus. *Antimicrobial Agents and Chemotherapy,57*(1), 83-95.

Casino, P., Rubio, V., & Marina, A. (2009). Structural Insight into Partner Specificity and Phosphoryl Transfer in Two-Component Signal Transduction. *Cell,139*(2), 325-336

Casino, P., Rubio, V., Marina, A. (2010). Mechanism of Signal Transduction by two component system,Current Opinion in Structural Biology, 20:763–771

Cui, L., Lian, J., Neoh, H., Reyes, E., & Hiramatsu, K. (2005). DNA Microarray-Based Identification of Genes Associated with Glycopeptide Resistance in Staphylococcus aureus. *Antimicrobial Agents and Chemotherapy,49*(8), 3404-3413.

Cui, L., Murakami, H., Kuwahara-Arai, K., Hanaki, H., & Hiramatsu, K. (2000). Contribution of a Thickened Cell Wall and Its Glutamine Nonamidated Component to the Vancomycin Resistance Expressed by Staphylococcus aureus Mu50. *Antimicrobial Agents and Chemotherapy, 44*(9), 2276-2285.

Diekema, D., Pfaller, M., Schmitz, F., Smayevsky, J., Bell, J., Jones, R., & Beach, M.

(2001). Survey of Infections Due toStaphylococcusSpecies: Frequency of Occurrence and Antimicrobial Susceptibility of Isolates Collected in the United States, Canada, Latin America, Europe, and the Western Pacific Region for the SENTRY Antimicrobial Surveillance Program, 1997–1999. *Clinical Infectious Diseases, 32*(S2).

Diensthuber, R., Bommer, M., Gleichmann, T., & Möglich, A. (2013). Full-Length Structure of a Sensor Histidine Kinase Pinpoints Coaxial Coiled Coils as Signal Transducers and Modulators. *Structure, 21*(7), 1127-1136.

Donaldson, L. W. (2008). The NMR Structure of theStaphylococcus aureusResponse Regulator VraR DNA Binding Domain Reveals a Dynamic Relationship between It and Its Associated Receiver Domain†. *Biochemistry,47*(11), 3379-3388.

Enright, M. (2003). The evolution of a resistant pathogen – the case of MRSA. *Current Opinion in Pharmacology, 3*(5), 474-479. doi:10.1016/s1471-4892(03)00109-7

Fan, X, Liu Y, Smith, D, Konermann L, Siu KW, Golemi-Kotra D. (2007). Diversity of penicillin-binding proteins. Resistance factor FmtA of *Staphylococcus aureus*. J Biol Chem. 282(48):35143-35152.

Foster, T. (1991). Potential for vaccination against infections caused by Staphylococcus aureus. *Vaccine, 9*(4), 221-227.

Gaddad, S., Thati, V., & Shivannavar, C. (2011). Vancomycin resistance among methicillin resistant Staphylococcus aureus isolates from intensive care units of tertiary care hospitals in Hyderabad. *The Indian Journal of Medical Research, 134*(5), 704.

Gao, R., & Stock, A. M. (2009). Biological Insights from Structures of Two-Component Proteins. *Annual Review of Microbiology, 63*(1), 133-154.

Gardete S, Wu SW, Gill S, Tomasz A. 2006. Role of VraSR in antibiotic resistance and antibiotic-induced stress response in *Staphylococcus aureus*. *Antimicrob AgentsChemother.* 50(10):3424-3434.

Gotoh, Y., Eguchi, Y., Watanabe, T., Okamoto, S., Doi, A., & Utsumi, R. (2010). Two-component signal transduction as potential drug targets in pathogenic bacteria. *Current Opinion in Microbiology, 13*(2), 232-239.

Gregory, P. D., Lewis, R. A., Curnock, S. P., & Dyke, K. G. (1997). Studies of the repressor (BlaI) of beta-lactamase synthesis in Staphylococcus aureus. *Molecular Microbiology, 24*(5), 1025-1037.

Grundmann, H., Aires-De-Sousa, M., Boyce, J., & Tiemersma, E. (2006). Emergence and resurgence of meticillin-resistant Staphylococcus aureus as a public-health threat. *The*

Lancet, 368(9538), 874-885.

Hafer, C., Lin, Y., Kornblum, J., Lowy, F. D., & Uhlemann, A. (2012). Contribution of Selected Gene Mutations to Resistance in Clinical Isolates of Vancomycin-Intermediate Staphylococcus aureus. *Antimicrobial Agents and Chemotherapy, 56*(11), 5845-5851

Ito, T., Okuma, K., Ma, X. X., Yuzawa, H., & Hiramatsu, K. (2003). Insights on antibiotic resistance of Staphylococcus aureus from its whole genome: genomic island SCC. *Drug Resistance Updates, 6*(1), 41-52.

Jung, K., Fried, L., Behr, S., & Heermann, R. (2012). Histidine kinases and response regulators in networks. *Current Opinion in Microbiology,15*(2), 118-124.

Kato, Y., Suzuki, T., Ida, T., and Maebashi, K. 2010. Genetic changes associated with glycopeptide resistance in *Staphylococcus aur- eus*: Predominance of amino acid substitutions in YvqF/VraSR. *J. Antimicrob. Chemother*. 65, 37–45.

Kernodle, D. S. (n.d.). Mechanisms of Resistance to β-Lactam Antibiotics. *Gram-Positive Pathogens, Second Edition,* 769-781. doi:10.1128/9781555816513.ch62

Konrad Plata1,2, Adriana E. Rosato2 and Grzegorz Węgrzyn1 ,2009 Vol. 56 No. 4/2009,

Koretke, K. K., Lupas, A. N., Warren, P. V., Rosenberg, M., & Brown, J. R. (2000). Evolution of Two-Component Signal Transduction. *Molecular Biology and Evolution, 17*(12), 1956-1970.

Kuroda, M., Kuroda, H., Oshima, T., Takeuchi, F., Mori, H., & Hiramatsu, K. (2004). Two-component system VraSR positively modulates the regulation of cell-wall biosynthesis pathway in Staphylococcus aureus. *Molecular Microbiology, 49*(3), 807-821.

Kuroda M, Ohta T, Uchiyama I, Baba T, Yuzawa H, Kobayashi I, Cui L, Oguchi A, Aoki K, Nagai Y et al. (2001). Whole genome sequencing of meticillin-resistant *Staphylococcus aureus*. Lancet. 357(9264):1225-1240.

Laub, M. T. (n.d.). The Role of Two-Component Signal Transduction Systems in Bacterial Stress Responses. *Bacterial Stress Responses, Second Edition,* 45-58.

Laub, M. T. and M. Goulian (2007). Specificity in two-component signal transduction pathways. *Annu Rev Genet 41*: 121-145

Leonard, P. G., Golemi-Kotra, D., & Stock, A. M. (2013). Phosphorylation-dependent conformational changes and domain rearrangements in Staphylococcus aureus VraR activation. *Proceedings of the National Academy of Sciences,110*(21), 8525-8530.

Lindsay, J. A., & Holden, M. T. (2004). Staphylococcus aureus: superbug, super genome? *Trends in Microbiology, 12*(8), 378-385

Liu, Y., Belcheva, A., Konermann, L., & Golemi-Kotra, D. (2009). Phosphorylation-Induced Activation of the Response Regulator VraR from Staphylococcus aureus: Insights from Hydrogen Exchange Mass Spectrometry. *Journal of Molecular Biology, 391*(1), 149-163

Lowy FD. 1998. *Staphylococcus aureus* infections agent overview of biochemistry and molecular genetics of its pathogenicity . N Engl J Med. 339(8):520-532.

Lowy, F. D. (2003). Antimicrobial resistance: the example of Staphylococcus aureus. *Journal of Clinical Investigation, 111*(9), 1265-1273.

Mascher, T., Margulis, N. G., Wang, T., Ye, R. W., & Helmann, J. D. (2003). Cell wall stress responses in Bacillus subtilis: the regulatory network of the bacitracin stimulon. *Molecular Microbiology, 50*(5), 1591-1604.

Mcphie, P. (2001). Circular Dichroism: Principles and Applications, Second ed. Edited by Nina Berova, Koji Nakanishi, and Robert W. Woody. *Analytical Biochemistry, 294*(2), 195.

Meehl, M., Herbert, S., Gotz, F., & Cheung, A. (2007). Interaction of the GraRS Two-Component System with the VraFG ABC Transporter To Support Vancomycin-Intermediate Resistance in Staphylococcus aureus. *Antimicrobial Agents and Chemotherapy,51*(8), 2679-2689.

Menon, S., & Wang, S. (2011). Structure of the Response Regulator PhoP fromMycobacterium tuberculosisReveals a Dimer through the Receiver Domain. *Biochemistry, 50*(26), 5948-5957.

Neoh, H., Cui, L., Yuzawa, H., Takeuchi, F., Matsuo, M., & Hiramatsu, K. (2007). Mutated Response Regulator graR Is Responsible for Phenotypic Conversion of Staphylococcus aureus from Heterogeneous Vancomycin-Intermediate Resistance to Vancomycin-Intermediate Resistance. *Antimicrobial Agents and Chemotherapy,52*(1), 45-53.

Pinho, M. G., Kjos, M., & Veening, J. (2013). How to get (a)round: mechanisms controlling growth and division of coccoid bacteria. *Nature Reviews Microbiology, 11*(9), 601-614.

Rammelkamp, C. H., & Maxon, T. (1942). Resistance of Staphylococcus aureus to the Action of Penicillin. *Experimental Biology and Medicine, 51*(3), 386-389.

Rhee, J. E., Sheng, W., Morgan, L. K., Nolet, R., Liao, X., & Kenney, L. J. (2008). Amino Acids Important for DNA Recognition by the Response Regulator OmpR. *Journal of Biological Chemistry, 283*(13), 8664-8677

Robinson,V.L.,Buckler, D.R., and Stock, A.M. (2000) A tale of two components: a novel kinase and a regulatory switch, *Nat.Struct.Biol.*7, 626 – 633

Ryan, K. J., Ray, C. G., & Sherris, J. C. (2004). *Sherris medical microbiology: an introduction to infectious diseases*. New York: McGraw-Hill.

Sengupta M, Jain V, Wilkinson, Jayaswal R, Can. J. (2012) Chromatin immunoprecipitation identifies genes under direct VraSR regulation in Staphylococcus aureus. *Microbiol*. 58: 703–708

Scheffers, D., & Pinho, M. G. (2005). Bacterial Cell Wall Synthesis: New Insights from Localization Studies. *Microbiology and Molecular Biology Reviews, 69*(4), 585-607.

Schito, G. (2006). The importance of the development of antibiotic resistance in Staphylococcus aureus. *Clinical Microbiology and Infection, 12*, 3-8.

Stapleton PD, Taylor PW. (2002) . Methicillin resistance in *Staphylococcus aureus*: mechanisms and modulation. Sci Prog. 85(Pt 1):57-72.

Walsh, T. R., & Howe, R. A. (2002). The Prevalence and Mechanisms of Vancomycin Resistance in Staphylococcus Aureus. *Annual Review of Microbiology, 56*(1), 657-675.

Yoo, J. I., Kim, J. W., Kang, G. S., Kim, H. S., Yoo, J. S., & Lee, Y. S. (2013). Prevalence of amino acid changes in the yvqF, vraSR, graSR, and tcaRAB genes from vancomycin intermediate resistant Staphylococcus aureus. *Journal of Microbiology,51*(2), 160-165. 7

Zhang, H. Z. (2001). A Proteolytic Transmembrane Signaling Pathway and Resistance to beta -Lactams in Staphylococci. *Science, 291*(5510), 1962-1965.

Zhang, H. Z. (2001). A Proteolytic Transmembrane Signaling Pathway and Resistance to beta -Lactams in Staphylococci. *Science, 291*(5510), 1962-1965.

Appendix A

Figure A1. The VraR wild type sequence and the DNA-sequencing blast result of VraR-E59D mutant. The highlighted red box represents the mutated bases.

ATGACGATTAAAGTATTGTTTGTGGATGATCATGAAATGGTACGTATAGGAATTTCAAGTTATC
TATCAACGCAAAGTGATATTGAAGTAGTTGGTGAAGGCGCTTCTGGTAAAGAAGCAATTGCCA
AAGCCCATGAGTTGAAGCCAGATTTAATTTTAATGGATTTACTTATG**GAA**GACATGGATGGTGT
AGAAGCGACGACTCAGATTAAAAAAGATTTACCGCAAATTAAAGTATTAATGTTAACTAGTTT
TATTGAAGATAAAGAGGTATATCGTGCATTAGATGCAGGTGTCGATAGTTACATTTTAAAAAC
AACAAGTGCAAAAGATATCGCCGATGCAGTTCGTAAAACTTCTAGAGGAGAATCTGTTTTTGA
ACCGGAAGTTTTAGTGAAAATGCGTAACCGTATGAAAAAGCGCGCAGAGTTATATGAAATGCT
TACAGAACGAGAAATGGAAATATTATTATTGATGCGAAAGGTTA**CT**CAAATCAAGAAATTGCT
AGTGCATCGCATATTACTATTAAAACGGTTAAGACACATGTGAGTAACATTTTAAGTAAGTTAG
AAGTGCAAGATAGAACACAAGCTGTCATCTATGCATTCCAACATAATTTAATTCAATAG

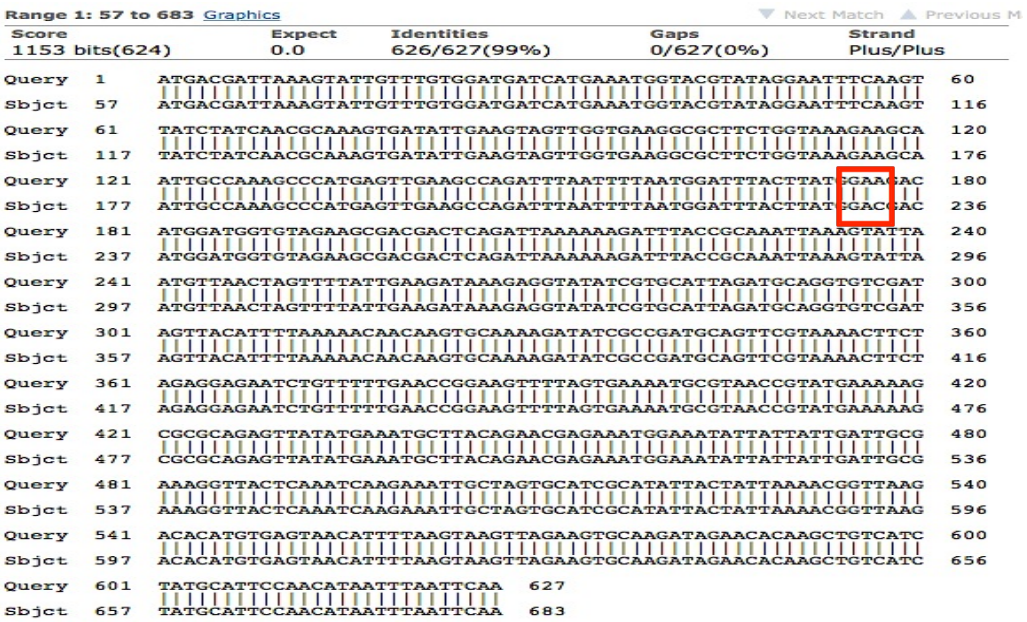

Appendix B

Figure B1 Raw data from vancomycin MIC experiment. The darker the box the higher is the OD_{600}.

Strains/ Vancomycin (µM)	2	1	0.5	0.25	0.125	0
RN4220	0.051	0.048	1.16	1.066	1.045	1.242
RN4220	0.047	1.309	1.461	1.493	1.517	1.457
RN4220ΔVraR	0.045	0.046	0.046	1.573	1.368	1.552
RN4220ΔVraR_(*vraR*::PMK4)	0.045	0.045	1.156	1.325	1.158	1.386
RN4220ΔVraR_(*vraR* M13A::PMK4)	0.053	0.047	0.613	0.886	1.196	1.184
RN4220ΔVraR_(vraR E59D::PMK4)	0.047	0.046	0.757	1.188	1.522	1.432
RN4220ΔVraR_(vraR S164P::PMK4)	0.049	0.048	0.049	0.953	1.317	1.333
RN4220ΔVraR_(vraR S164A::PMK4)	0.049	0.046	0.651	1.217	1.241	1.357